Research Square

Preprints are preliminary reports that have not undergone peer review.
They should not be considered conclusive, used to inform clinical practice,
or referenced by the media as validated information.

Impact of Climate Change and Anthropogenic Stresses on the Spatio-Temporal Variability of River-Aquifer Exchanges

Ranveer Kumar

ranveerkumar.rs.civ20@iitbhu.ac.in

Indian Institute of Technology BHU

Shishir Gaur

Indian Institute of Technology BHU

Anurag Ohri

Indian Institute of Technology BHU

Research Article

Keywords: River Aquifer Exchanges, Climate Change, Groundwater Sustainability, Baseflow Depletion

Posted Date: September 1st, 2026

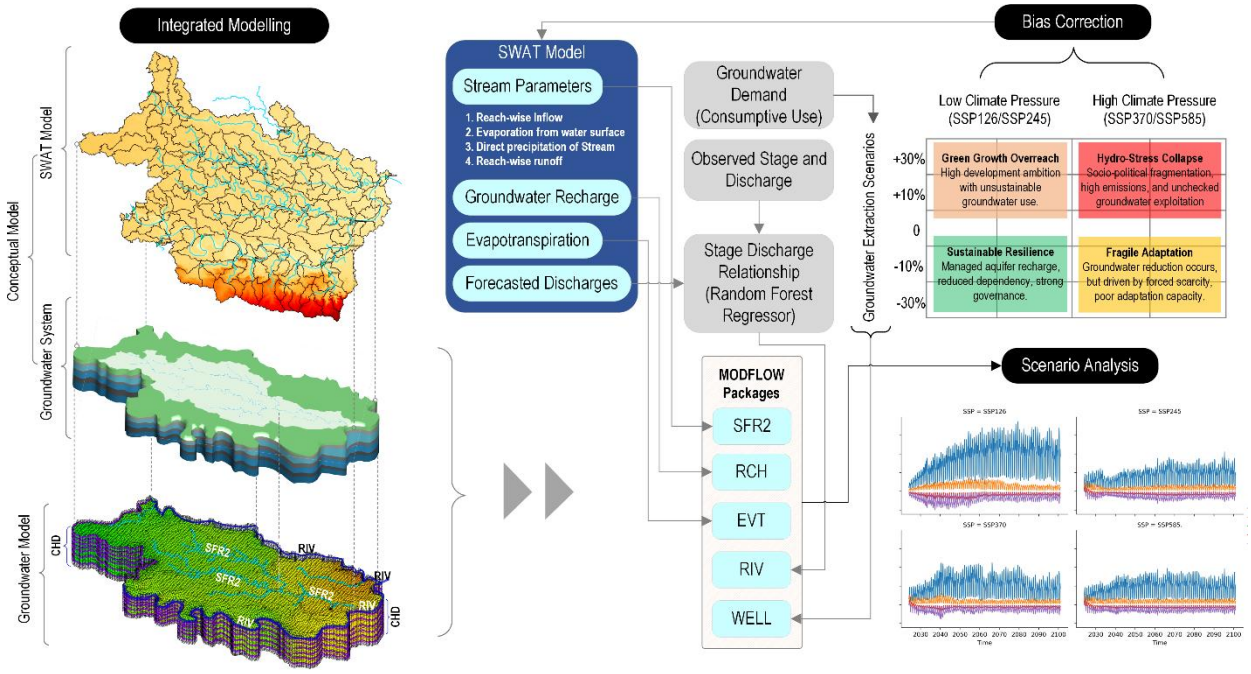
DOI: https://doi.org/10.21203/rs.3.rs-10719084/v1

License: This work is licensed under a Creative Commons Attribution 4.0 International License.
Read Full License

Additional Declarations: No competing interests reported.

Impact of Climate Change and Anthropogenic Stresses on the Spatio-Temporal Variability of River-Aquifer Exchanges

Graphical Abstract:



Abstract:

River-aquifer exchanges (RAE) are critical for river health but are increasingly threatened by climate change and groundwater extraction, particularly in alluvial systems like the Varuna River Basin (VRB). This study quantifies the spatio-temporal dynamics of RAE in the VRB and assesses the combined impacts of future climate (CMIP6-SSPs) and anthropogenic (groundwater extraction) stresses. An integrated modeling framework was developed, coupling SWAT and MODFLOW, and was calibrated using both groundwater heads and Differential Flow Gauging data to accurately simulate low-RAE system. Twenty future scenarios have been analyzed within a four-quadrant socio-environmental framework, and its impact on the spatio-temporal dynamic

of baseflow and river aquifer connectivity (net gaining and loosing river reaches). The results revealed that groundwater extraction is the most dominant driver of RAE dynamics. Increased pumping severely degrades river connectivity, while reduced pumping offers a robust mitigation strategy. The system's response to climate change was found to be complex and heterogeneous, challenging simplistic assumptions and validating the necessity of integrated modeling. The findings highlight that direct management of groundwater abstraction is the most effective lever for building hydrological resilience, as unchecked extraction, even under milder climate scenarios, will accelerate the river's decline toward losing its dry-season flow.

Keywords: River Aquifer Exchanges, Climate Change, Groundwater Sustainability, Baseflow Depletion

1 INTRODUCTION

Exchanges between rivers and aquifers play a critical role in the sustainability of groundwater-fed rivers. These interactions are essential for sustaining water availability, as they maintain groundwater levels and streamflow (Konrad, 2006; Wöhling et al., 2018). This connectivity ensures a continuous water supply to the river, which is essential for sustaining ecosystems during dry periods (Ronayne et al., 2017). The hyporheic zone, where river water and groundwater (GW) mix, is a crucial ecotone that supports a variety of biological communities and ecological processes. This zone serves as a refuge for aquatic organisms and plays a significant role in nutrient cycling and the transformation of organic matter (Brunke and Gonser, 1997; Ellis et al., 2007). River-aquifer exchanges (RAE) affect the distribution and abundance of aquatic species by creating habitats with stable temperatures and nutrient availability (Brunke and Gonser, 1997; Krause et al., 2012). These exchanges facilitate the natural attenuation of contaminants such as

nitrates through denitrification processes in the hyporheic zone. This is particularly important for maintaining water quality in the river and the adjacent aquifer (Bartsch et al., 2014; Macdonald et al., 2018). Given the vital role of RAE in maintaining river sustainability, understanding the impacts of climate change and groundwater abstractions is essential for developing effective water management strategies to adapt to future ecological challenges (Carolli et al., 2017; Chunn et al., 2019; Taylor et al., 2013).

The processes of RAE demonstrate significant variability in response to hydrological conditions, including precipitation events and levels of river discharge (Bartsch et al., 2014; Unland et al., 2015). Shallow aquifer-fed rivers exhibit rapid and seasonally variable responses to hydrological signals, with attenuation of short-term fluctuations but clear transmission of longer-term trends. The specific response depends on aquifer-river connectivity, natural groundwater recharge, and local geology, making these systems sensitive indicators of both climate variability and RAE (Lu et al., 2021). Given that the natural groundwater recharge is highly dependent on the local climatic conditions, climate change has a profound impact on RAE, particularly in arid regions with limited water resources. Higher temperatures generally increase evapotranspiration, leading to reduced baseflow, while changes in precipitation can either mitigate or amplify these effects, depending on regional conditions (Hu et al., 2023a; Li et al., 2021; Miller et al., 2021; Xiang et al., 2021). These effects also vary seasonally and spatially, with some regions experiencing increased streamflow during wetter months and reduced baseflow during drier periods (Hu et al., 2023a, 2023b).

To sustain the growing population in India, groundwater extraction can significantly impact natural RAE processes, resulting in diminished connectivity, modification of flow regimes, and potential degradation of water quality (Ellis et al., 2007; Jasechko et al., 2021). Aggravated by anthropogenic activities, climate change has an adverse impact on the hydrological regime of a

river (Ren et al., 2025). The increased intensity due to climate change leads to flooding events in the rainy season and dry channels in the lean season (Gaur et al., 2023). Increased rainfall intensity often leads to more surface runoff and less infiltration, reducing groundwater recharge (Jan et al., 2007). In India, the impact of rainfall intensity on groundwater recharge varies by region. In the northwest and north-central regions, low-intensity rainfall is more beneficial for recharge, whereas in the Southern part of India, high-intensity rainfall drives natural recharge (Asoka et al., 2018). The combined effects of reduced recharge and increased groundwater extraction in India have resulted in a declining groundwater trend, consequently diminishing the baseflow to groundwater-fed rivers (Cooper et al., 1995; Mukherjee et al., 2018). This underscores the need for region-specific insights into baseflow dynamics and rainfall–aquifer exchange (RAE) patterns, particularly in the face of climate change and increasing groundwater demand. By addressing these complexities at the basin scale, this research offers a novel and timely contribution to the field.

For climate change impact assessment, the quantification of river–aquifer exchange (RAE) is generally conducted using analytical and empirical methods based on observed streamflow data, such as recursive digital filters, the conductivity mass balance approach, and various algorithmic techniques (Zhang et al., 2013). However, these methods are often limited by data availability and their low parameterization to represent the RAE processes. With advances in computational capabilities, transient groundwater models can be highly parameterized to capture complex hydrogeological conditions and provide detailed insights into baseflow dynamics. For instance, a fully integrated surface water–groundwater flow model has been shown to reproduce baseflow behavior that can serve as a benchmark for evaluating automated baseflow separation techniques (Partington et al., 2012). By employing systematic and explicit parameterization strategies to capture heterogeneous hydraulic properties, numerical models can better represent reality, leading

to more reliable and less uncertain outcomes (Cui et al., 2021). Further, due to limited streamflow data availability, the baseflow separation methods cannot be used in rivers with limited gaging stations, such as the Varuna River Basin (VRB). To achieve accurate reach-wise estimates of RAE and hence the baseflow, we advanced the previous methodology of climate change impact assessment on baseflow of a river by projecting the distributed climate change signals from Global Circulation Models (GCMs) to groundwater-surface water dynamics.

The RAE flux in alluvial rivers such as VRB is lower compared to the streamflow and not detectable by seepage meters. This makes it difficult to get accurate estimates of RAE in heterogeneous aquifer media (Tang et al., 2017, 2015). The well-calibrated GW models are used by several researchers to simulate the reach scale RAE (Bajpai et al., 2023; Baratelli et al., 2016; Vergnes and Habets, 2018). However, these models are generally calibrated using groundwater heads, which makes the estimated RAE uncertain. Differential flow gaging (DFG) data can be a powerful tool for calibrating groundwater models, especially for quantifying exchanges in rivers with lower RAE flux. By comparing streamflow gain and losses between different sections, the fluxes between rivers and aquifers can be directly estimated, providing critical constraints for model calibration (McCallum et al., 2014; Mccallum et al., 2012; Schilling et al., 2019).

While DFG appears to be a useful tool for calibrating the groundwater models for river–aquifer exchanges quantification, its reliability decreases in systems with low exchange fluxes. In such cases, changes in streamflow between gauging stations are often minimal and may be masked by measurement uncertainties, evaporation losses, or unaccounted tributary inflows and outflows. This makes it difficult to distinguish actual groundwater interactions from background noise, leading to high uncertainty in flux estimates (Mccallum et al., 2012), especially in lower parameterized MODFLOW packages for RAE simulation (e.g. RIV, STR). To solve this, the SFR2

package (Niswonger & Prudic, 2005) offers detailed parameterization to explicitly account for evaporation losses, as well as inflows from direct precipitation and surface runoff. Incorporating SFR2 into the groundwater model can help reduce uncertainties associated with reach-scale inflows and outflows in river systems (Vasilevskiy et al., 2022), thereby enabling the use of DFG data for groundwater model calibration. Given the limited literature on calibrating groundwater models with DFG data, this study presents a novel approach to improve model accuracy in simulating river-aquifer exchanges (RAE).

In this study, we developed a fully calibrated, highly parameterised groundwater model to quantify reach-wise river–aquifer exchanges (RAE) under climate change in the Varuna River Basin (VRB). The model integrates downscaled and bias-corrected outputs from four CMIP6 climate scenarios (SSP126, SSP245, SSP370, SSP585) with five groundwater extraction scenarios to assess current and future RAE dynamics under changing climate and anthropogenic stress. Hydrological fluxes simulated by SWAT were coupled with MODFLOW and calibrated using observed groundwater heads and DFG data. Different baseflow determination methods were compared, highlighting the advantage of the integrated modeling approach for rivers with low baseflow index (BFI). This framework provides a novel and robust means to evaluate spatio-temporal river-aquifer interactions in changing climate and groundwater extraction, bridging a methodological gap in groundwater-surface water assessment and offering critical insights for groundwater sustainability in river approaching hydrological disconnection from adjacent alluvial aquifers in Varuna River Basin (Mishra et al., 2024). The specific objectives are as follows:

i. Integration of climate model outputs, physically based hydrological model and 3D numerical groundwater model to simulated river aquifer exchanges.

ii. Parameterization and calibration of heterogeneous aquifer properties and river-bed hydraulic conductivity using observed heads and DFG data

iii. Simulating spatiotemporal variability of baseflow and river aquifer connectivity for different climate change and groundwater demand scenarios in VRB.

2 STUDY AREA

The Varuna River has a total basin area of 3,664.6 km², originating from Dain Tal and joining the mighty Ganga near the sacred city of Varanasi. The river system, including its tributaries Basuhi and Morwa, extends over a total length of 550 km (derived using SRTM Digital Elevation Model) and supports a population of approximately six million people. The region receives an average annual rainfall of 872.8 mm and average temperature varies between 7 – 47℃, based on data from 2003 to 2023.

The basin is predominantly composed of older alluvium, while areas closer to the Ganga feature younger alluvial deposits. The loamy soil in the region is highly fertile, with nearly 87% of the land dedicated to agriculture. The principal *rabi* crops include wheat and oilseeds, whereas paddy and pulses dominate the *kharif* season. Groundwater serves as the primary source of potable water for domestic consumption, and approximately 87.5% of the region's irrigation needs are met through tube wells.

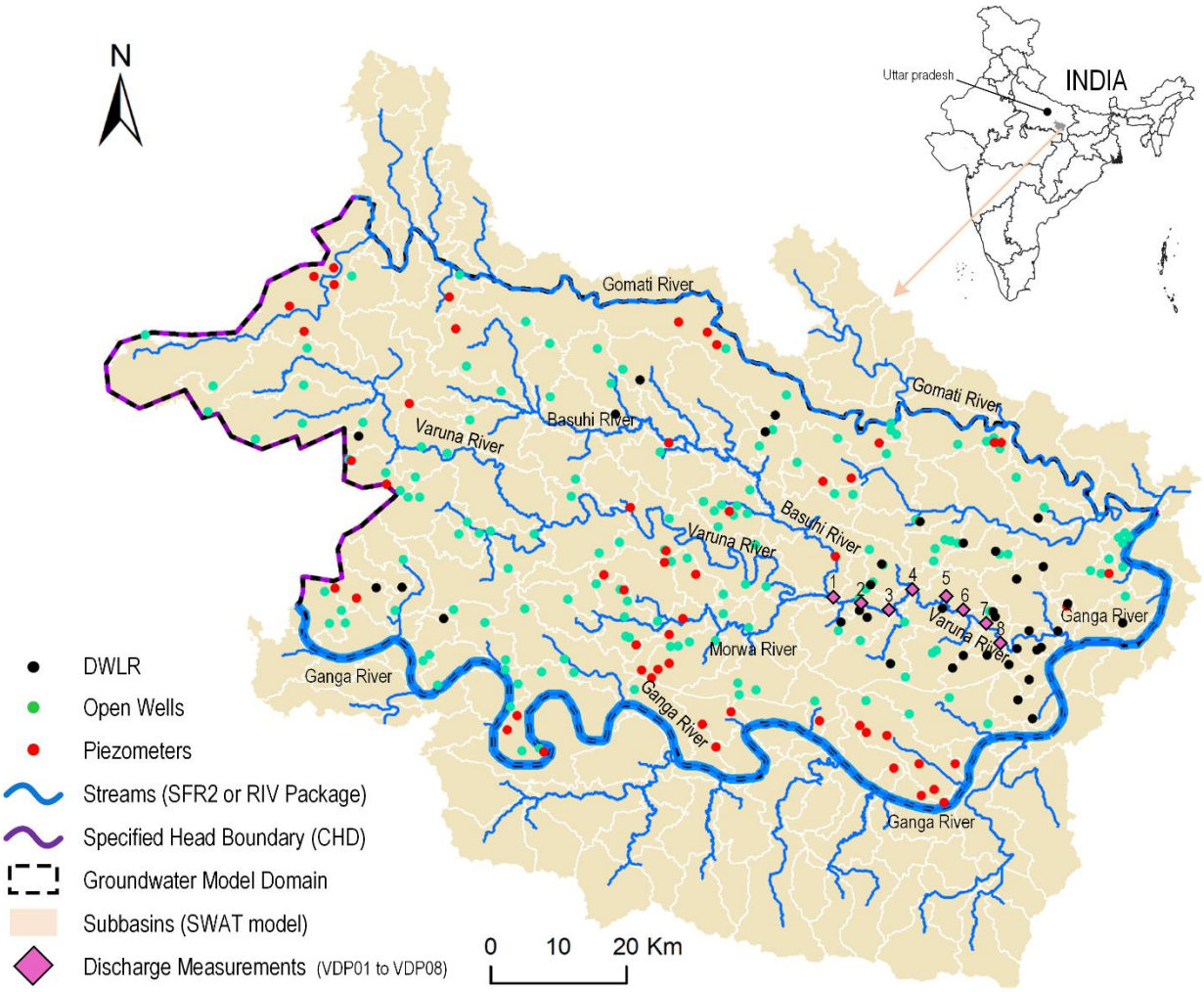


Figure 1.Study Area representing groundwater model domain with boundary conditions (DWLR: digital water level recorder)

The Varuna River basin is experiencing a marked decline in river flow and a deterioration of water quality, primarily due to increased groundwater extraction, urbanization, agricultural intensification, and the direct discharge of untreated sewage and industrial waste. Studies reveal that the river water is moderately to highly polluted, with elevated levels of biological oxygen demand (BOD), chemical oxygen demand (COD), nitrates, and other contaminants, largely attributed to sewage inflow, excessive fertilizer use, and poor waste management practices (Kumar

and Agrawal, 2025; Singh and Singh, 2010). Groundwater in the basin, while generally suitable for irrigation, is increasingly threatened by nitrate and fluoride contamination, posing health risks, especially to children, and reflecting the leaching of agricultural chemicals and inadequate sanitation infrastructure (Dey et al., 2023; Janardhana Raju et al., 2009). The shrinking and siltation of natural ponds and tanks have further reduced the basin's capacity to buffer floods and support groundwater recharge, exacerbating both water scarcity and quality issues (Kumar et al., 2025; Mishra et al., 2024). Collectively, these factors underscore the urgent need for integrated water management strategies to restore river flow and improve water quality in the Varuna River basin.

3 MATERIAL AND METHODOLOGY

3.1 Differential Flow Gauging (DFG)

Differential flow gauging has been used to calculate the loss or gain of stream flow with the surrounding GW. The methodology is based on the water balance for the river reach:

$$Q_{in} + Q_t + Q_g + R + Q_r = Q_{out} + Q_d + ET + \frac{\Delta S}{\Delta t} \quad (1)$$

Where Q_{in} is inflow at the upstream of the reach, Q_t is the inflow from tributaries and point sources, Q_g is the GW flux to the river reach, R is the direct rainfall on the water surface, Q_r is the runoff inflow to the stream, Q_{out} is the outflow from the river reach at the downstream end, Q_d is the flow out from the reach due to diversions and canal feeder pumps, ET is the evapotranspiration from the river reach and $\frac{\Delta S}{\Delta t}$ is the change in river bank storage with time. All the component of equation (1) has the unit of discharge (L^3T^{-1}).

In the case of no tributary and point sources in the study reach, the inflow and outflow components of the water balance are zero. So, the seepage flux at time *t* between two gauged sections with a total wetted area A_w is given as-

$$RAE_t = \frac{Q_{out,t} - Q_{in,t} - R_t - Q_{r,t} + ET_t}{A_w} \quad (LT^{-1}) \tag{2}$$

3.2 Comparison of baseflow determination methodologies

The selection of suitable baseflow determination method for the climate change assessment has been done based on the agreement with observed baseflow at VDP08 during dry period. The baseflow has been determined by observing the gain/loss in the eight sections (VDP01 to VDP08 in **Figure 1**) during dry flow periods with Acoustic Doppler Current Profiler (ADCP) (Sonotek-M9).

Four methodology (three baseflow separation method and MODFLOW-based approach) which is widely used, has been compared to determine the baseflow time series with observed flow at VDP08. The key parameters of the baseflow separation methods have been calibrated with the observed baseflow at VDP08 by DFG.

3.2.1 Eckhardt Filter

The Eckhardt filter (Eckhardt, 2008) is a widely used recursive digital filter for baseflow separation, relying on two key parameters: the recession constant (α) and the maximum baseflow index (BFImax). This method effectively distinguishes baseflow from total streamflow by attenuating high-frequency stormflow signals, producing hydrologically plausible results across diverse catchments and time steps (Helfer et al., 2024).

3.2.2 Local Minima Method

The local minima method is a graphical approach that identifies baseflow by connecting the lowest points (local minima) on a streamflow hydrograph, assuming these points represent periods dominated by groundwater contributions. This method is straightforward, easy to implement, and requires minimal data, making it accessible for rapid assessments or in regions with limited resources (Helfer et al., 2024).

3.2.3 BFI Method

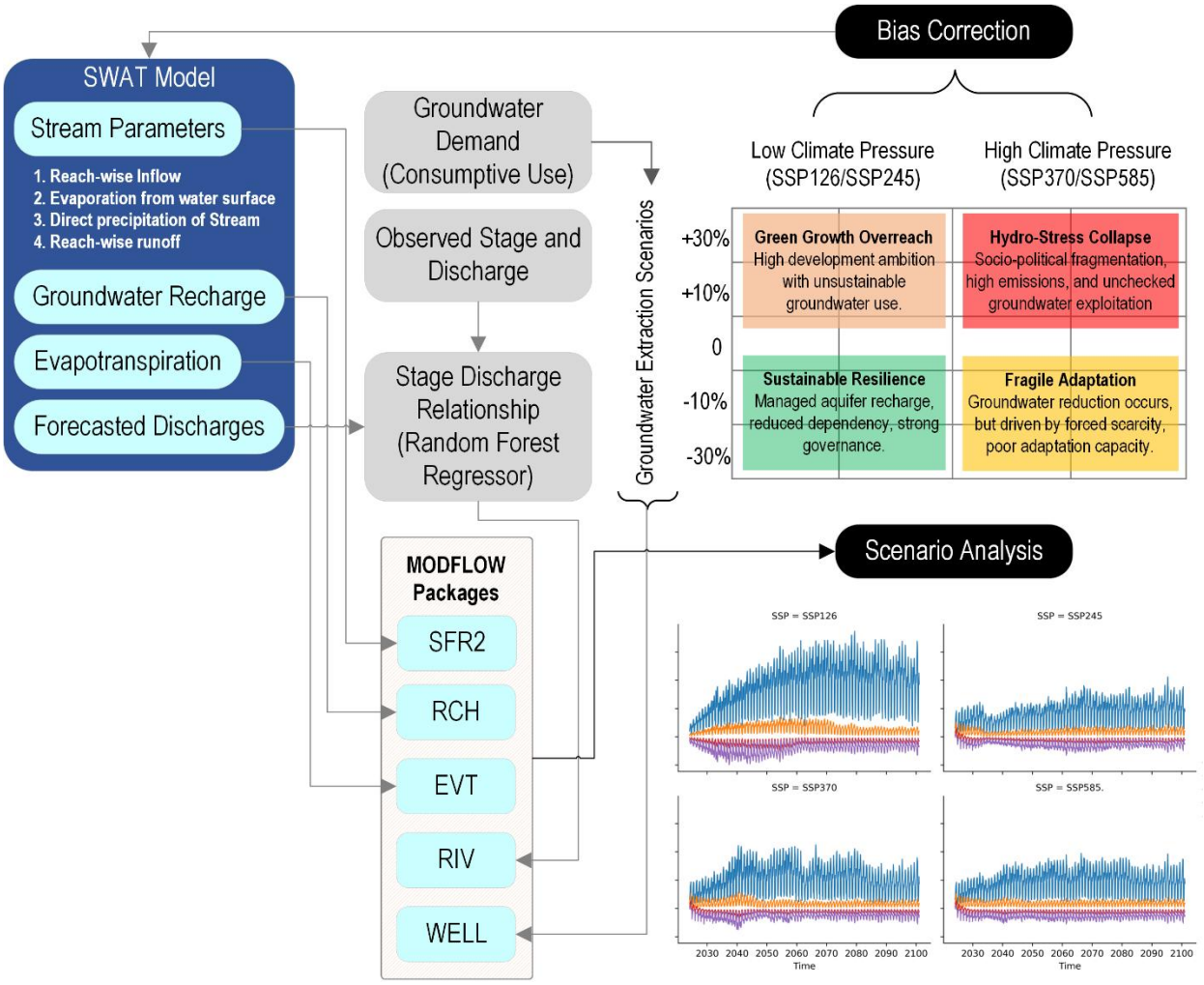
The Baseflow Index (BFI) method quantifies the proportion of baseflow in total streamflow over a given period, often using digital filters or graphical separation techniques to estimate the baseflow component. BFI estimates depends heavily on the underlying separation method and parameterization, which can introduce uncertainty and variability in results, especially in heterogeneous or data-limited environments (Sun et al., 2021).

3.2.4 Numerical Model-Based Calculation

Numerical model-based baseflow determination uses finite difference models (such as MODFLOW) to simulate RAE. This approach allows for detailed, scenario-based analysis and can incorporate spatial and temporal variability, making it suitable for complex or large-scale studies. However, these models require extensive data, careful calibration, and validation, and their complexity can introduce additional sources of error or uncertainty if not properly managed (Xie et al., 2024; Zhang et al., 2020).

3.3 Modelling the hydrology of the area

The simulation of climate change impact on the groundwater system is a double-loop feedback system, where the attribution signals start from climate parameters and reflect on the surface water fluxes, moving further to the groundwater. The Soil Water Assessment Tool (SWAT) has been used to simulate the first cascading effect of climate change on the surface water hydrology in Varuna River Basin. The following paragraphs briefly summarize the SWAT modelling under a climate change scenario, and the readers are encouraged to follow the comprehensive methodology in Kumar et al. (2025).



230

231 **Figure 2**. Overall methodology for surface water and groundwater integration and scenario analysis

232

233 The model domain for the SWAT model has been chosen in such a way that it encapsulates the
234 groundwater model extent (**Figure 1**) governed by the two major rivers – Ganga and Gomati.
235 Various streams of datasets used for the conceptualization of the SWAT model for the study area
236 are presented in Kumar et al. (2025). A total of 185 subbasins have been delineated with a total
237 of 2506 HRUs (Hydrological Response Units). The weather variables (Rainfall and Temperature)
238 have been taken from daily IMD 2D gridded dataset. The model has been simulated with daily
239 timestep from year 2020 to year 2024 including 2 years of warmup period. The daily streamflow

observation at seven gaging stations (five on Ganga, one on Gomati, and one on Varuna River) has been used for the calibration and validation of the SWAT model. After satisfactory calibration of the model, the weather variables from the four CMIP6 scenarios have been used for further simulations to determine the climate change signals to the hydrological fluxes. For simulating the climate change, the monthly time-steps has been used to avoid a computationally expensive model. The HRU-scale (Evapotranspiration, Recharge) and the reach-scale hydrological variables (Runoff coming to the reach, Evaporation from the reach, Rainfall directly falling on the reach and the inflow-outflow) from the SWAT model, have been used for further conceptualize the groundwater model in MODFLOW.

3.4 Integration of SWAT model outputs to MODFLOW-NWT

To model the second feedback loop, the outputs from the hydrological model has been used as input for the groundwater model. The climate change signals have been transferred to the groundwater model with MODFLOW-packages (EVT, RCH and RIV) to ensure accurate simulations. The Varuna River has been modeled with highly parametrized SFR2 Package, taking outputs from the reach-wise SWAT outputs (*'output.rch'*). The Evapotranspiration and Recharge at the top surface has been taken from the '*output.hru*', resampled at subbasin scale for easy input to the MODFLOW' RCH and EVT packages. The detailed modelling steps have been presented in **Figure 2** and described in the **supplementary material**.

The GW model has been discretized in 750m uniform square grids, seven layers and 14 days' time steps. The forecasting model consists of monthly time steps. The models hydraulic conductivity (K_h) and specific storage (Ss) have been calibrated to fit the 1101 observed groundwater heads at multiple time steps using PEST (Doherty, 2015). The K_h and Ss for the seven layers have been

parameterized by uniformly distributed pilot-points (equally separated by 5 Km). The river bed hydraulic conductivity has been parameterized based on the sub-basin reaches (total 57 reaches). After getting the first set of calibrated aquifer K_h and Ss values, the river bed hydraulic conductivity of 57 reaches in Varuna River has been calibrated to fit the observed gain and loss by DFG at the eight river sections (**Figure 1**). This method improved the simulation of river flow and the contribution of RAE. The fitted river bed K_h has been used again as fixed parameter to calibrate the aquifer K_h and Ss. This calibration loop has been performed four times to get the desired fit of GW head (R^2= 0.81) and observed differential flow (R^2=0.71). The fitted aquifer properties and the river bed hydraulic conductivity can be found in the **Appendix A** and **B** of the supplementary material.

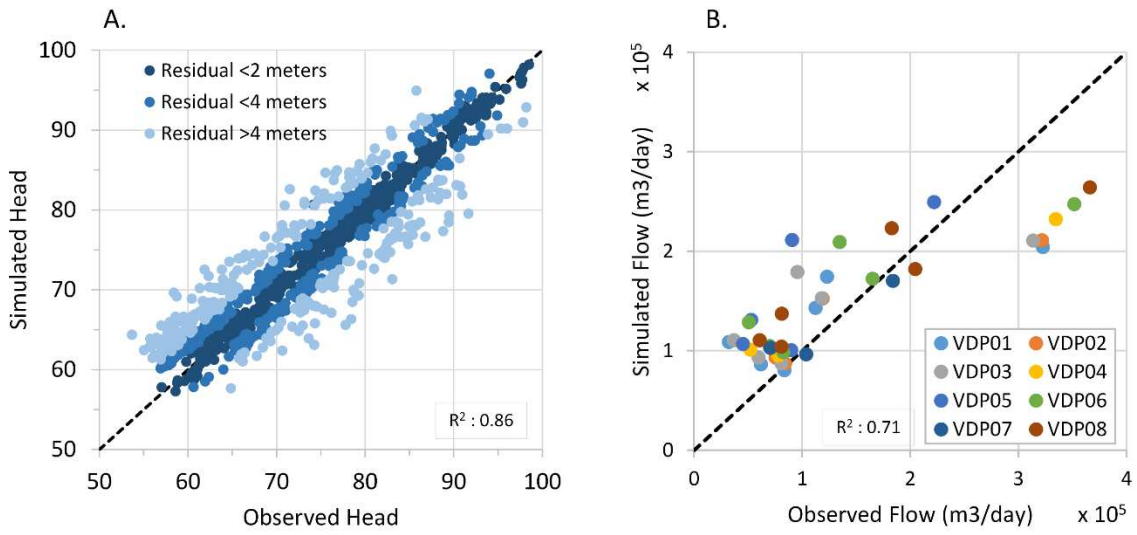


Figure 3. Simulated vs. calibrated scatter plot for A. observed heads and B. observed stream flow.

3.5 Model Uncertainty

Uncertainty analysis is critical in groundwater modeling because inherent challenges like spatial heterogeneity, sparse observational data, and parameter non-uniqueness can lead to overconfident deterministic predictions that obscure potential risks in water resource management. The PESTPP-IES addresses this by implementing an iterative ensemble smoother to perform computationally efficient history matching and uncertainty quantification for highly parameterized GW models. To accomplish this, PESTPP-IES evaluates an ensemble of parameter realizations representing the prior probability distribution and iteratively updates them to match historical observations, transforming them into a posterior ensemble that reflects both calibrated parameters and predictive uncertainty. A primary advantage of this methodology is its computational efficiency: the number of forward models runs required per iteration depends only on the number of ensemble realizations, rather than the thousands of parameters comprising each realization. This approach allows hydrogeologists to rigorously assess probabilistic capture zones, evaluate low-probability risks, and condition parameters in high-dimensional systems without suffering from computational burden (Doherty, 2015; White et al., 2020).

After determining the calibrated prior with PEST, the uncertainty of the GW model has been analyzed using PESTPP-IES. To save the computational time, only three layers (layer 1, 3, 5) has been parameterized for Kh and two layer (Layer 3, 5) for Ss. The lower limit for Kh for all layers has been 0.1 m/day and the upper limit were 1000, 2500 and 3500 m/day respectively. The limit for Ss has been taken as 10^{-7} to 0.001. A total 450 realization has been explored with 30% subset for lambda updates. The PESTPP-IES has been run for five iterations. The base realization of the posterior has been used further as predictor for climate change and anthropogenic stresses impact on the RAE.

3.6 Climate change and anthropogenic stress scenarios

To assess the combined effect of climate change and anthropogenic stress on the groundwater system, the four SSP and five population growth cases have been considered. The population growth has been calculated with logistic growth method with base scenario of population corresponding to the carrying capacity of two billion for whole Indian subcontinent (Daily and Ehrlich, 2016). The carrying capacity of the study area has been determined based on the ratio of total population in the Varuna River Basin (~6 million) to the total current population of India. This comes out to be 1.54 times the current population of the VRB (i.e. ~9.24 million). The average growth rate of Uttar Pradesh from 2001 to 2011 was 2.02% per year. Based on these data, the population demand was forecasted, assuming that agricultural activity will require more or less the same amount of water while domestic demand will increase logistically (Kumar et al., 2025). The forecasted population demand has been used as the baseline GW extraction for the VRB. Four other GW demand scenario has been created by increasing/decreasing the demand by 10% and 30% from the baseline.

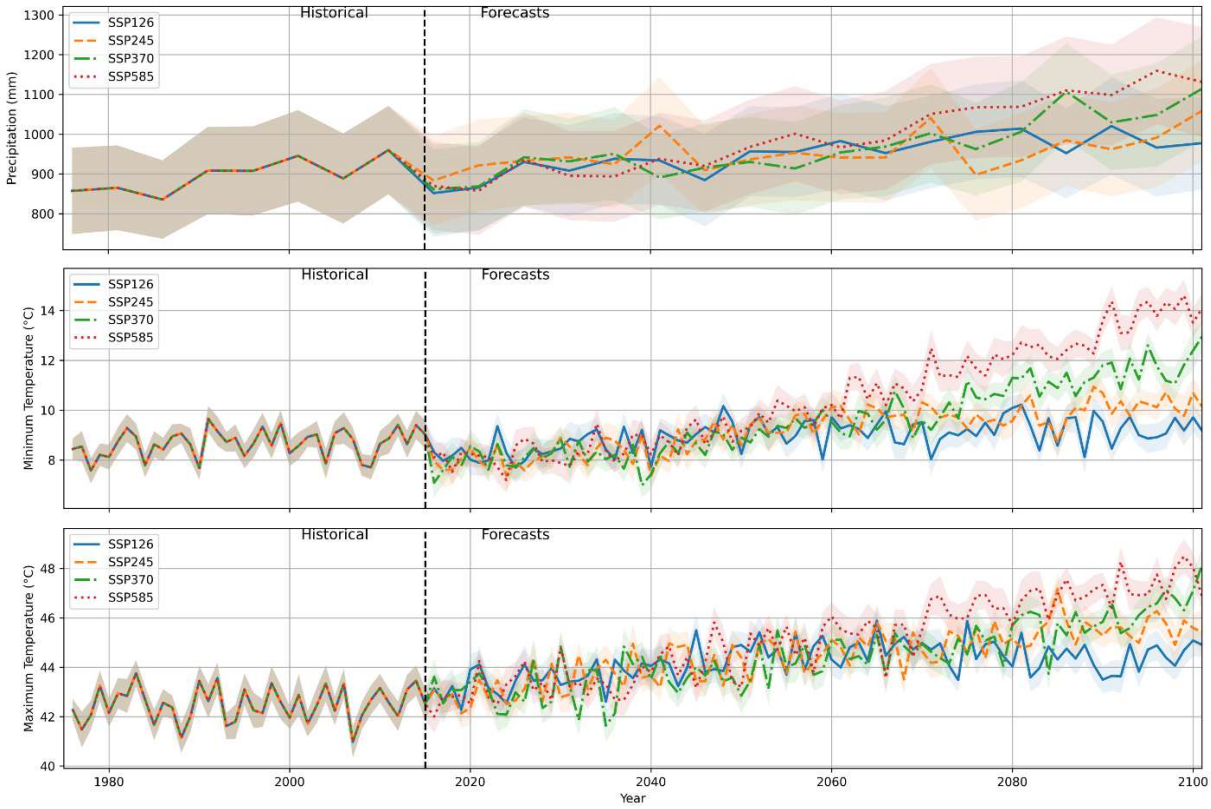


Figure 4. The projected climate variables in VRB (The data has been plotted as annual averages to create smooth plots. The precipitation data is 5-year average data, and the temperature data are annual minimum or maximum.)

To assess the impact of climate change, this study utilized climate data from the Coupled Model Intercomparison Project Phase 6 (CMIP6). Recognizing that raw General Circulation Model (GCM) outputs have coarse spatial resolutions and inherent biases, a statistical downscaling and bias-correction procedure was implemented using machine learning algorithms. Specifically, a Random Forest Regressor (RFR) was used to correct maximum and minimum temperature variables, while a Long Short-Term Memory (LSTM) model was applied to the more stochastic precipitation data. These models were trained against high-resolution gridded data from the India Meteorological Department (IMD) to ensure accuracy. Following an evaluation of 21 GCMs, the ten best-performing models were selected, and their outputs were averaged to generate a robust climate dataset for four Shared Socioeconomic Pathway (SSP) scenarios (**Figure 4**).

The downscaled and bias-corrected climate variables for each SSP scenario were subsequently integrated into the calibrated SWAT model. This integration enabled a comprehensive assessment of the basin's hydrological response to various climate change. For a detailed explanation of the downscaling, bias-correction, and model integration methodology, readers are encouraged to follow the procedures outlined in Kumar et al. (2025).

Based on the four climate and five GW extraction scenario, a total 20 GW models have been prepared satisfying four broad sustainability scenarios (**Figure 2**).

- **Sustainable Resilience**
    - Low climate pressure and a significant decrease in groundwater extraction (-10% to -30%).
    - In a future with milder climate change, humanity acts wisely. We reduce our dependency on groundwater, and actively replenish aquifers (managed recharge) to ensure long-term water security. This is the most desirable and stable outcome.
- **Green Growth Overreach (The Unsustainable Boom)**
    - Low climate pressure but a significant increase in groundwater extraction (+10% to +30%).
    - Society aims for high economic and social development ("Green Growth"), but fuels this ambition by unsustainably pumping too much groundwater. While the climate is manageable, this over-extraction puts the system under stress and is not a viable long-term strategy. It's a case of good intentions leading to resource depletion.
- **Hydro-Stress Collapse**

- High climate pressure and a significant increase in groundwater extraction (+10% to +30%).
- Faced with severe climate change, society breaks down ("socio-political fragmentation"). There is no coordinated effort to manage resources, leading to unchecked exploitation of groundwater as a last resort. This combination of a harsh climate and resource depletion leads to a societal collapse driven by water stress.

- **Fragile Adaptation**
  - High climate pressure and a decrease in groundwater extraction (-10% to -30%).
  - In this scenario, groundwater use is reduced, but not because of good planning. Instead, the reduction is forced by extreme scarcity, the water is simply running out due to climate impacts. Society has a poor capacity to adapt, and this is a reactive, unstable state of survival rather than a planned, resilient future. The adaptation is "fragile" because it's born out of crisis, not strategy.

3.7 Baseflow Index and Reach Characteristic

The assessment criteria for all the scenario have been presented with the baseflow index (BFI). BFI represents the ratio of flow contribution from groundwater to the total stream flow at a section. The baseflow is the sum of all the reach-scale loss and gain of water, when a river interacts with adjacent aquifer. The "net baseflow" in this study represents the net RAE, which can be negative, distinguishing it from traditional hydrograph separation outputs. The baseflow dynamics under changing climatic and GW extraction scenarios has been determined using the twenty numerical model simulations as discussed above.

The spatio-temporal dynamics for the given scenarios have been determined based on the reach-wise statistics of net influx to and outflux from the river to the adjacent aquifer. The statistics on the length of gaining and loosing stream has also been assessed under the given scenarios. The trend analysis of each assessment parameter (reach length, influx/outflux) has been performed with the sen's slope method.

3.8 Error metrics

There are two error metrices, that has been used in the research work to assess the model calibration and comparison of different baseflow determination methods.

$$R^2 = \left[\frac{\sum_{i=1}^{n}(o_i - \bar{o}_i)\,(p_i - \bar{p}_i)}{\sqrt{\sum_{i=1}^{n}(o_i - \bar{o}_i)^2}\,\sqrt{\sum_{i=1}^{n}(p_i - \bar{p})^2}}\right] \quad (3)$$

$$RMSE = \sqrt{\frac{1}{n}\sum_{i=1}^{n}(o_i - p_i)^2} \quad (4)$$

Given that p_i is the predicted/simulated value corresponding to the actual/observed value o_i , $\bar{o}_i$ is the actual/observed mean and $\bar{p}_i$ is the mean of predicted/simulated values.

4 RESULTS AND DISCUSSION

4.1 Parameter and predictive uncertainty of the GW model

4.1.1 Objective function convergence and predictive uncertainty

The minimization of the global objective function (Phi) across the ensemble is detailed in **Figure 5**.A. The observation weights were in range from 1.54 to 2.68, which was assigned based on the standard deviation and respective uncertainty due to methodology employed for observation (manual measurements got higher weight compared to DWLRs). The ensemble mean Phi decreased from an initial, unconditioned prior value of 110,564 to a final posterior value of 72,614, showing a total decrease of 34.34%. he standard deviation and the absolute min-max bounds of the ensemble narrowed considerably by Iteration 5. This progressive constriction indicates that the parameter realizations were successfully updated to respect historical observations, effectively minimizing global model misfit while preserving a realistic band of uncertainty.

Figure 5.B highlights a dramatic shift in the global head residuals. The prior residual distribution was highly dispersed and multimodal, with errors spanning broadly from -10 to +10 meters. Post-assimilation, the posterior residual density collapsed into a tight, near-Gaussian distribution centered precisely on the zero-error line, indicating the removal of systematic bias and a high degree of confidence in the calibrated predictions. **Figure 5**.C reinforces this by plotting the posterior simulated heads against the observed data. The ensemble means cluster tightly along the 1:1 reference line.

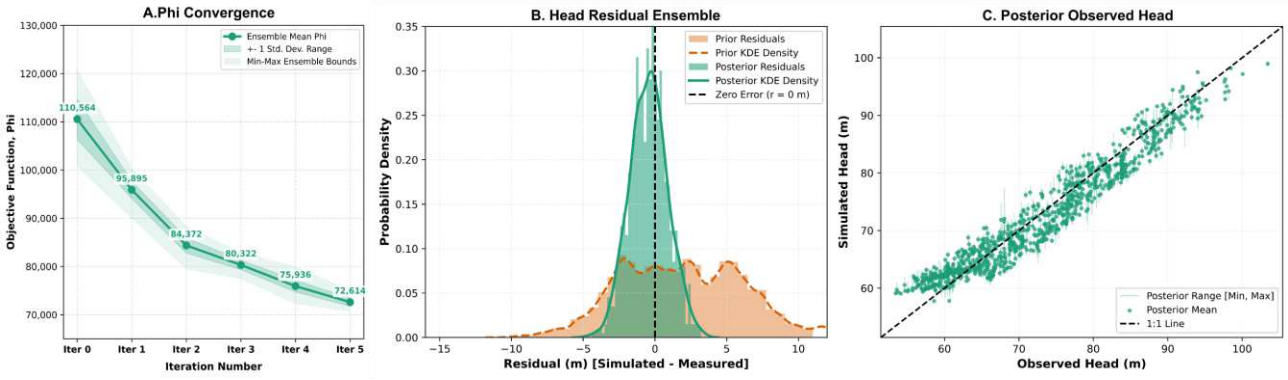


Figure 5. A. Objective function (phi) convergence across five iterations; B. Prior and Posterior observation residual ensemble; C. Posterior simulated head vs observed head

4.1.2 Parameter Conditioning and Non-Uniqueness

While the predictive outputs show high confidence, the posterior parameter distributions underscore the inherent non-uniqueness of the groundwater system **Figure 6**. Plot (a) through (e) contrast the prior and posterior Probability Density Functions (PDFs) for hydraulic conductivity (*Kh*) and specific storage (*Ss*) across Layers 1, 3, and 5. The posterior distributions exhibit refined, sharpened peaks compared to their broad prior counterparts, demonstrating effective parameter conditioning. Plot (f) quantifies this parameter-level conditioning via the standard deviation reduction of the ensemble. The median uncertainty reduction consistently exceeds 70% across most parameter groups, with *Kh* in Layer 1 demonstrating the highest median reduction at 85.5%.

Despite substantial statistical reduction, multimodality and spread persist in several posterior PDFs (e.g., the secondary peaks in *Kh* for Layers 1 and 5). This indicates that while the ensemble can accurately replicate historical heads, multiple distinct parameter combinations can yield equivalent model fits. This residual spread accurately characterizes the remaining parameter uncertainty, proving that PESTPP-IES maintained appropriate epistemic variance rather than overfitting to a single deterministic parameter field.

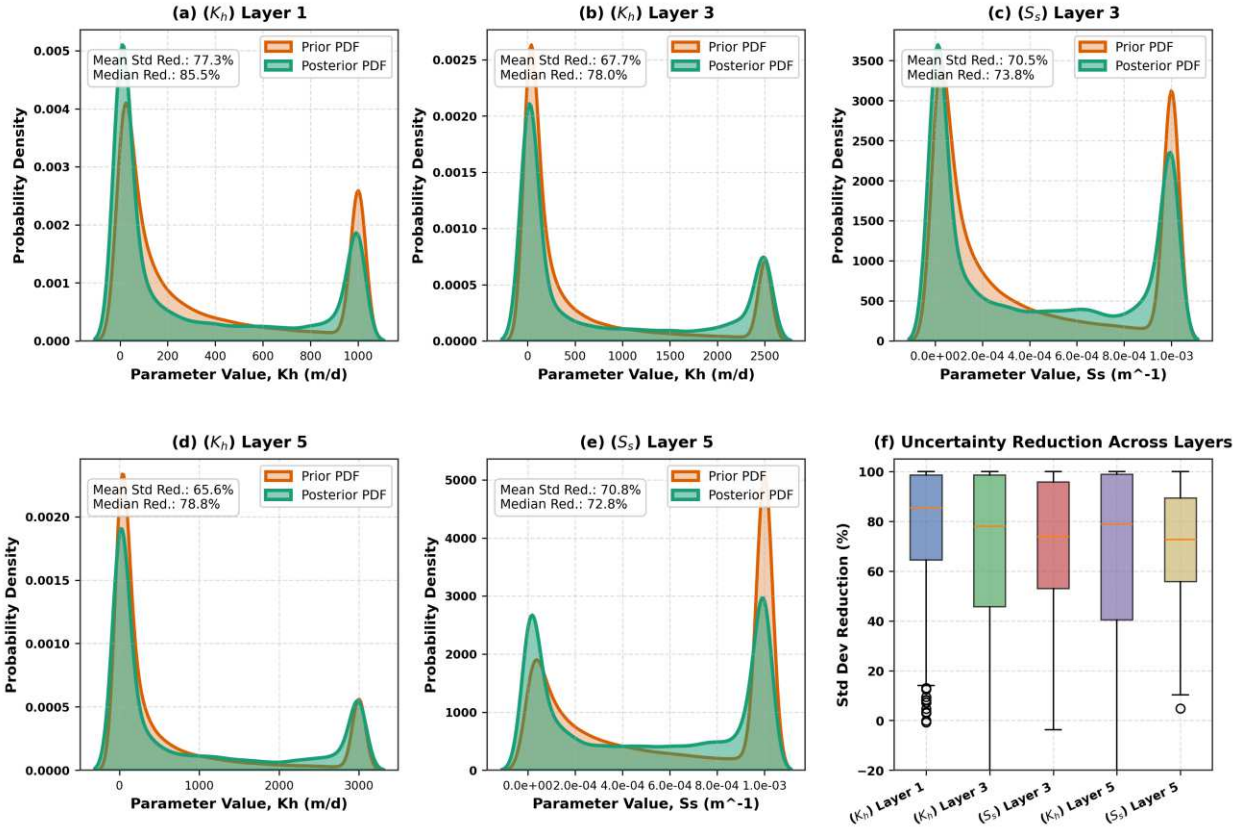


Figure 6. Posterior parameter distribution and total uncertainty reduction.

4.2 RAE dynamics of Varuna River Basin

4.2.1 Calculation and comparison with baseflow-separation methodology

The contribution from the upstream reaches in Varuna River during the dry period has been assumed to be minimal (disconnection of stream and the aquifer) and the dry flow at VDP01 (~ 0.1 to 0.3 m^3/sec) has been taken as the initial flow in the stream. The assumption is supported by the distribution of major point sources, located upstream of VDP01 or downstream of VDP08, with active RAE occurring downstream of VDP01. Consequently, this river segment was chosen

for analysis. The baseflow at VDP08 was determined by summing the reach-scale losses and gains between VDP02 and VDP08 (represented by five observed baseflow data as markers in **Figure 7**).

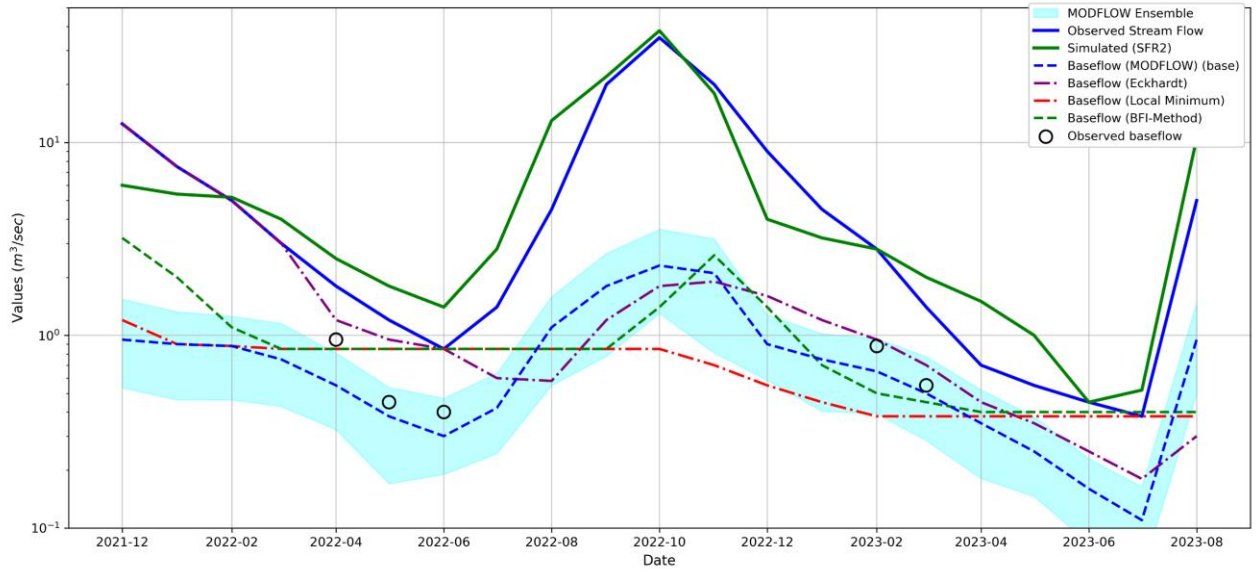


Figure 7. Comparison of simulated flow and baseflow determined using various methods (The values are determined for VDP08)

The difference between the actual baseflow and the dry flow observed during the field campaigns can be observed in **Figure 7** (represented with markers and blue solid line respectively). As illustrated, conventional baseflow separation methods (e.g., Eckhardt, BFI-Method) failed to capture the actual baseflow measured during field campaigns (represented by markers). This discrepancy is caused by unaccounted sewer discharges, which lead to calibration errors in baseflow separation methods. Similarly, when calibrated to total streamflow, SWAT compensates for these unknown point sources by erroneously overestimating the groundwater contribution (baseflow). To overcome this limitation, we utilized an integrated modeling approach. The robust surface process parameters from SWAT (surface runoff and evaporation) were integrated into the SFR2 package, and the baseflow has been simulated with MODFLOW-NWT.

The integrated model effectively simulates total streamflow (green vs. blue line) and reproduces baseflow with high accuracy. The base realization (and the posterior ensemble) from MODFLOW simulation aligns closely with observed data, quantitatively supported by a Root Mean Square Error (RMSE) of 0.201 m^3/day, markedly lower than that obtained using conventional methods.

4.2.2 Gaining and Losing Reach

The spatio-temporal analysis of the exchange flux in the Varuna River for the current simulation period (2022-23) indicates that for most of its length, particularly the upstream reach from 0 to approximately 160 km, the river consistently loses water to the alluvial aquifer. This leakage, though generally low in intensity, signifies a continuous recharge of groundwater by the river. The downstream reach, from 160 km to its confluence with the Ganga, is the zone of most intense hydrogeological interaction. This section is characterized by significant, large-scale water loss from the river to the aquifer. However, counteracting this dominant trend are highly localized gaining reaches (positive flux), identifiable as distinct red hotspots.

Superimposed on this spatial pattern is a strong seasonality that dictates the temporal variability of baseflow generation. These critical gaining reaches (stream leakage >250 m^3/day), which constitute the sole source of the river's baseflow, are spatially insignificant, comprising less than 5% of the river's total length. The activity of these hotspots is also temporally dynamic; their flux is most pronounced during the dry season and the post-monsoon recession period (approximately October to May). During this time, as the overall river stage falls, the hydraulic gradient from the localized, high-potential aquifer allows for a strong and sustained discharge into the channel. Conversely, during the peak monsoon, high river stage suppresses this influx. This fundamentally reframes the understanding of baseflow in the Varuna system, indicating that it is not a widespread

contribution but is instead a highly localized phenomenon, active primarily outside of the main monsoon period.

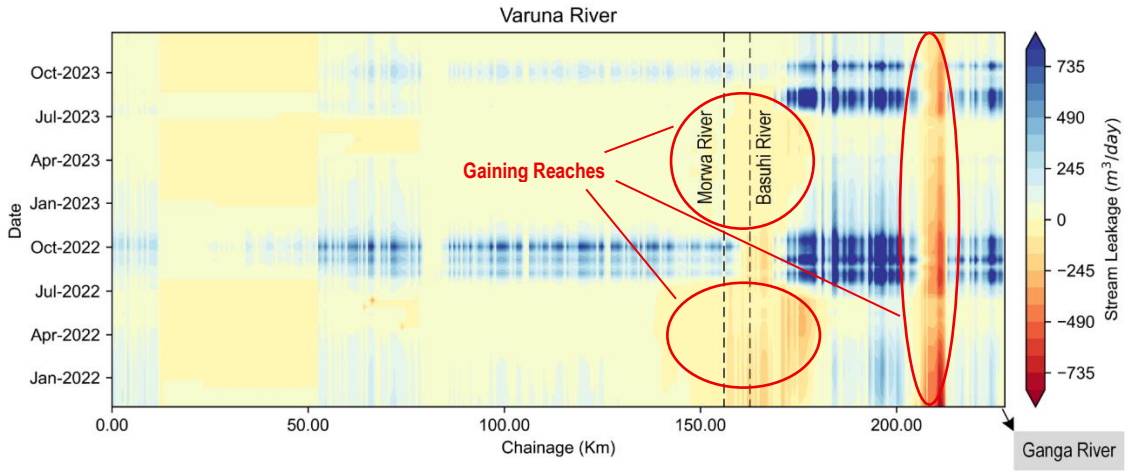


Figure 8. The spatiotemporal dynamics of river aquifer exchanges (stream leakage) in Varuna River (excluding the Basuhi and Morwa reaches). The +ve stream leakage is associated with loosing river sections and vice versa.

4.3 Impact on Baseflow: Extraction supersedes the climate change

4.3.1 Baseflow Index under climate change

Figure 8 shows that the Varuna River is predominantly losing, with the net outflow to the aquifer (sum of all positive reach-scale RAE) exceeding the inflow (sum of all negative reach-scale RAE). Traditionally, the Baseflow Index (BFI) is defined as the ratio of baseflow to total streamflow, and thus, it's typically a positive value ranging from 0 to 1. This range of analysis has been constraint by the methodology applied to determine the baseflow, which was based on hydrograph separation. The reach-wise quantification of RAE has opened an opportunity to analyse the net baseflow which can be negative if the river is primarily losing.

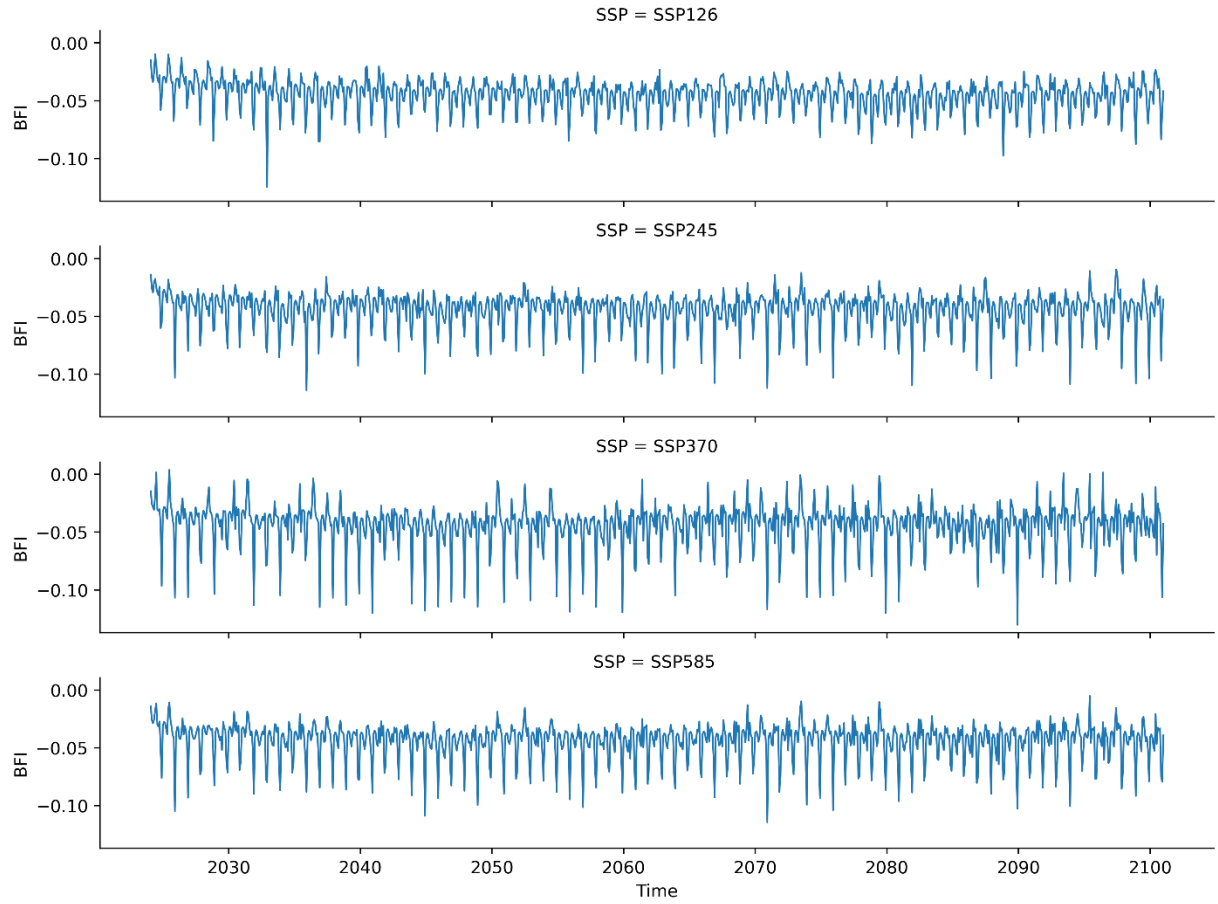


Figure 9. The variation of BFI with climate change along the four SSPs.

The consistently negative BFI values indicate that the Varuna River is projected to largely function as a losing stream, recharging the underlying aquifer. The fluctuations, where BFI becomes closer to zero, likely correspond to periods of increased precipitation and groundwater recharge (the seasonality in the plot), temporarily reducing the rate of water loss from the river to the aquifer, or even briefly creating a gaining condition (**Figure 9**). The long-term implication, especially with increasing temperatures and decreasing recharge (Kumar et al., 2025), is a heightened risk of streamflow depletion and reduced ecological flows as the river continues to lose water to the groundwater system.

499

500 *4.3.2 Overall BFI under Groundwater Extraction Scenarios*

501 The BFI for the Varuna River has been analysed from a "Business as Usual" (BAU) scenario,
502 where groundwater extraction rates remain constant at current levels (2021-2023) throughout the
503 projection period (2025-2100). This deviation is examined across four Shared Socioeconomic
504 Pathways (SSPs: SSP126, SSP245, SSP370, SSP585) and four alternative groundwater abstraction
505 (GWD) scenarios, which represent ±10% and ±30% changes relative to the BAU extraction rate,
506 calculated using a logistic growth method. The Y-axis quantifies this deviation in cubic meters per
507 day (m^3/day) (**Figure 10**).

508 Under scenarios of increased groundwater abstraction, a consistent and significant reduction in
509 river baseflow relative to the BAU scenario is observed across all SSPs. For the +10% GWD
510 scenario, baseflow consistently deviates negatively, typically ranging from approximately -0.0005
511 m^3/day to -0.001 m^3/day. This depletion is exacerbated in the +30% GWD scenario, where
512 deviations are markedly more negative, generally falling between -0.0015 m^3/day and -0.002
513 m^3/day. These negative deviations are prevalent for the projection period of (2025-2100),
514 highlighting that increased pumping directly diminishes the groundwater contribution to river
515 flow. While the overall pattern of depletion is robust across SSPs, there are subtle modulations;
516 for instance, under the higher emission scenario SSP585, the negative deviations sometimes appear
517 slightly more pronounced, suggesting a compounding effect where increased climatic stress (e.g.,
518 higher evapotranspiration) potentially exacerbates pumping-induced baseflow reduction.

519 Conversely, implementing strategies that reduce groundwater abstraction from BAU levels
520 consistently leads to an increase in river baseflow. In the -10% GWD scenario, baseflow deviations
521 are positive, generally ranging from approximately +0.0005 m^3/day to +0.001 m^3/day. This

positive impact is significantly amplified in the -30% GWD scenario, with baseflow deviations frequently reaching between +0.004 m³/day and +0.007 m³/day, particularly towards the latter half of the century. Notably, these positive deviations often exhibit an increasing trend over time, especially under lower emission SSPs (e.g., SSP126, SSP245), suggesting that a combination of reduced pumping and projected climatic changes (such as increased precipitation effectiveness) can lead to a substantial and sustained enhancement of river baseflow.

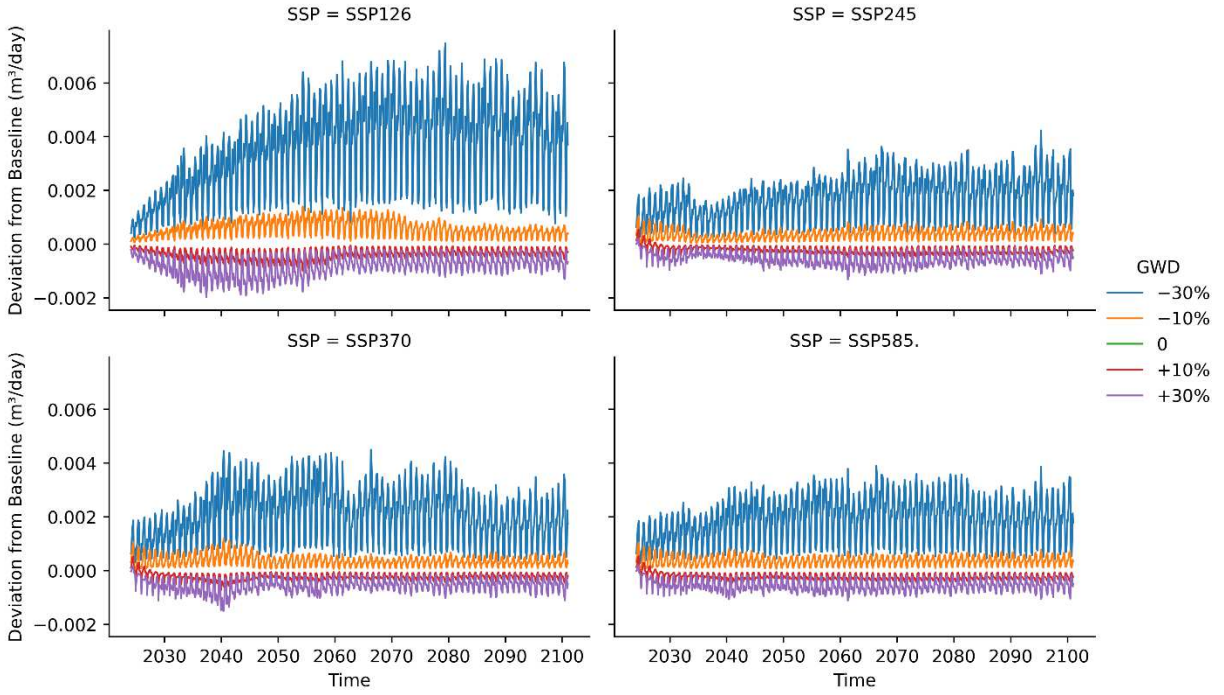


Figure 10. The increase/decrease in the BFI with respect to BAU for all SSPs

4.4 Gaining and Losing Reaches

It is cumbersome to understand the overall impact of climate change on the baseflow, especially when the value is -ve. To better understand the combined impact of climate and GW stress, we analysed the response of gaining and loosing reaches separately.

4.4.1 Net Influx to the Varuna River

The net inflow to Varuna River has been interpreted with the detailed statistics of River-Aquifer Exchange (RAE) influx and total gaining reach length from the raster plots (**Figure 11**) within the context of four defined future quadrants: "Green Growth Overreach," "Hydro-Stress Collapse," "Sustainable Resilience," and "Fragile Adaptation" (**Figure 2**). This quadrant integrates climate pressure (Low: SSP126/SSP245; High: SSP370/SSP585) and groundwater extraction scenarios (ranging from -30% to +30% relative to a Business As Usual baseline). This structured approach allows for a clearer understanding of the combined impact of climatic and anthropogenic pressures on the Varuna River's hydrological status.

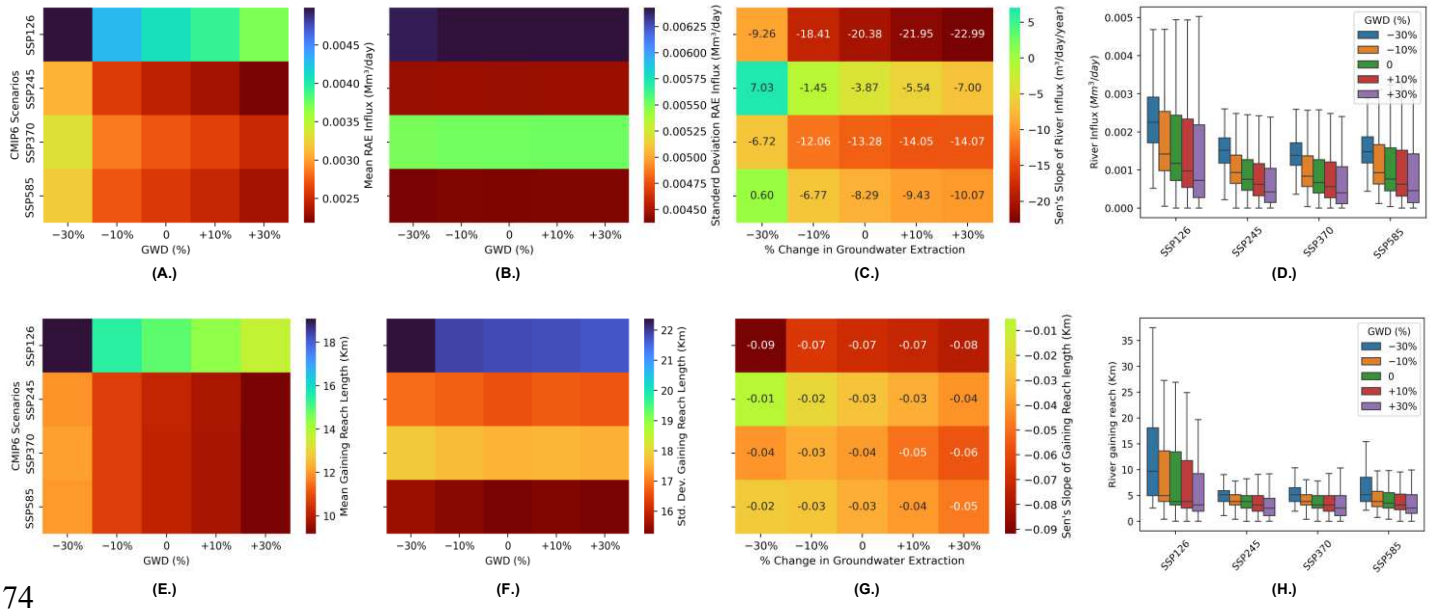
I. Green Growth Overreach:

This quadrant represents futures characterized by low climate pressure (SSP126/SSP245) but with high development ambition and unsustainable groundwater use (+10% or +30% GWD). Under these conditions, the raster plots (**Figure 11**.A, C, E, G) indicate a significant deterioration of river-aquifer interactions despite relatively benign climate conditions. Mean RAE influx is projected to decrease substantially from the BAU baseline, ranging from -0.0005 to -0.001 Mm^3/day for +10% GWD and -0.0015 to -0.002 Mm^3/day for +30% GWD compared to the zero-change baseline. Similarly, the mean gaining reach length shows clear reductions. Crucially, the Sen's Slope analysis reveals consistent negative trends for both RAE influx (e.g., ~-22.9 m^3/day/year under SSP126/+30% GWD in **Figure 11**.C and **Figure 12**) and gaining reach length (e.g., ~-0.08 km/year under SSP126/+30% GWD in **Figure 11**.G). This demonstrates that even with mild climate change, unchecked groundwater exploitation critically undermines river baseflow and connectivity, leading to a rapid decline in the river's ecological health.

558

559 **II. Hydro-Stress Collapse**:

560 This quadrant depicts a future of high climate pressure (SSP370/SSP585) combined with
561 continued or increased groundwater exploitation (+10% or +30% GWD), indicative of
562 socio-political fragmentation and unchecked resource use. Within this scenario, the raster
563 plots show the most severe and alarming impacts on the Varuna River. Mean RAE influx
564 (**Figure 11**.A) consistently falls to its lowest values (approaching 0.003 Mm^3/day under
565 SSP585/+30% GWD), with mean gaining reach lengths (**Figure 11**.E) similarly at their
566 shortest (around 16 km under SSP585/+30% GWD). The long-term trends are
567 overwhelmingly negative but lower than previous scenario and often the most pronounced.
568 For instance, the Sen's Slope for RAE influx (**Figure 11**.C) reaches its most negative values
569 (e.g., -10.07 m^3/day/year under SSP585/+30% GWD), indicating a rapid and accelerating
570 depletion of groundwater contribution to the river. This scenario forecasts a future where
571 compounded pressures from severe climate change and unsustainable abstraction lead to
572 extensive hydrological disconnection, severe baseflow depletion, and a collapse in the
573 river's natural supporting functions.



574

575 **Figure 11**. Scenario plots based on the Figure 2; Top row represents the statistics (A. Mean, B. Standard
576 deviation, C. Sen's Slope/trend and D.summary box plots) for RAE influx; The bottom row represents the
577 statistics (E. Mean, F. Standard deviation, G. Sen's Slope/trend and H.summary box plots) for total gaining reach
578 length of Varuna River.

579

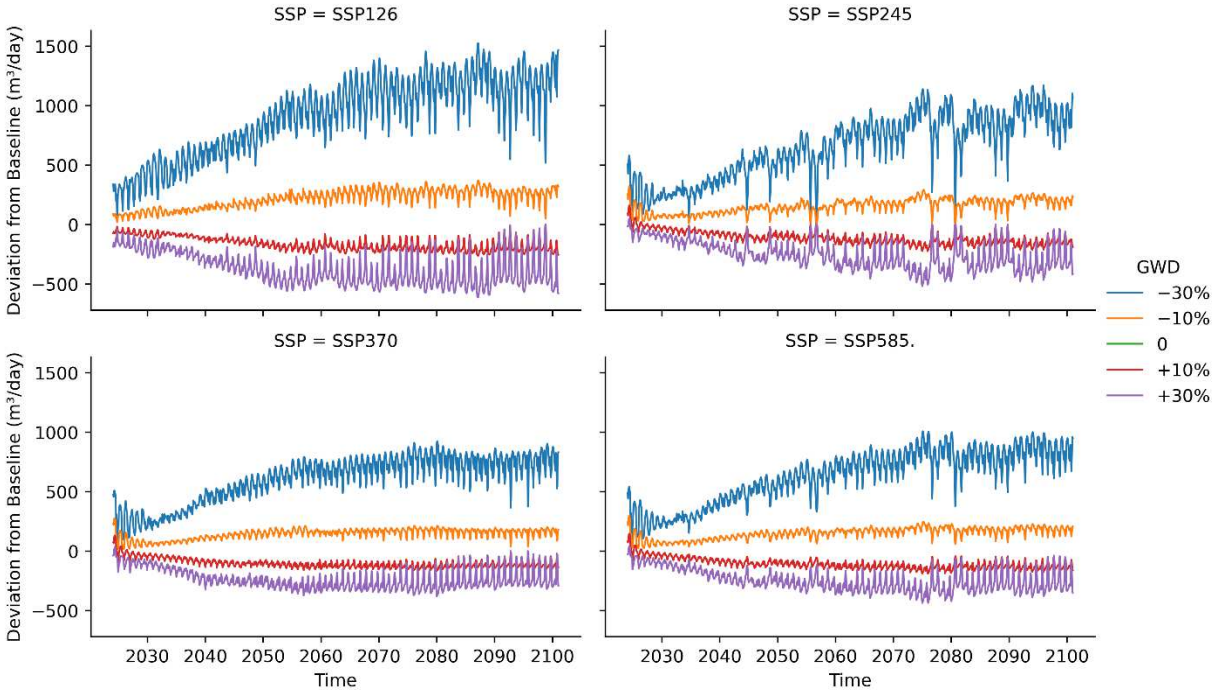
580 **III. Sustainable Resilience**:

581 This quadrant represents a highly desirable future with low climate pressure
582 (SSP126/SSP245) combined with proactive groundwater management strategies, such as
583 managed aquifer recharge, reduced dependency, and strong governance (-10% or -30%
584 GWD). Under these optimal conditions, the raster plots illustrate the most beneficial
585 outcomes for the Varuna River's hydrological integrity. Mean RAE influx (**Figure 11**.A)
586 reaches its highest values (e.g., ~0.0045 Mm^3/day under SSP126/-30% GWD), and mean
587 gaining reach length (**Figure 11**.E) is at its longest (e.g., ~22 km under SSP126/-30%
588 GWD). Crucially, this quadrant shows the only consistently positive long-term trends for
589 both RAE influx (e.g., 5.94 m^3/day/year under SSP126/-30% GWD in **Figure 11**.C) and
590 gaining reach length (e.g., 0.09 km/year under SSP126/-30% GWD in **Figure 11**.G). This

indicates that strategically reducing groundwater abstraction under milder climate change allows the river-aquifer system to not only maintain but actively improve its connection and groundwater contribution over time, fostering true hydrological resilience.

IV. Fragile Adaptation:

This quadrant portrays a future with high climate pressure (SSP370/SSP585) where groundwater reduction occurs, but is potentially driven by forced scarcity and poor adaptation capacity (-10% or -30% GWD). While abstraction is reduced, the benefits are somewhat tempered by the challenging climate context. Mean RAE influx (**Figure 11**.A) and mean gaining reach length (**Figure 11**.E) are generally higher than in the high abstraction quadrants, benefiting from reduced pumping. For example, under SSP585/-30% GWD, mean RAE influx is around 0.0035 Mm^3/day and mean gaining reach length is around 18 km. However, the long-term trends (**Figure 11**.C, G) are often neutral or only slightly positive (e.g., ranging from ~-0.77 to ~2.89 m^3/day/year for RAE influx trends, and around 0.00-0.03 km/year for gaining reach length trends), unlike the strong positive trends seen in "Sustainable Resilience." This indicates that while reduced groundwater exploitation helps to mitigate the negative impacts of severe climate change, the high climatic pressure limits the extent to which the river-aquifer system can recover or improve. Adaptation in this scenario is fragile, as the system struggles to regain robust hydrological health despite human efforts.



611

612 **Figure 12.** The increase/decrease in the net influx to the Varuna River with respect to BAU for all SSPs

613

614 *4.4.1 Outflux from the Varuna River*

615 The outflux from the river is highly dependent on the hydraulic gradient with respect to the
616 adjacent aquifer. As high-intensity rainfall events become more frequent due to climate change, as
617 reported in numerous studies worldwide (Gaur et al., 2023; Kumar et al., 2024), the duration of
618 river flow decreases, leading to reduced seepage into aquifers. The net outflow from Varuna River
619 has been interpreted simillarily as influx, represented with the scenario plots (**Figure 13**).

620

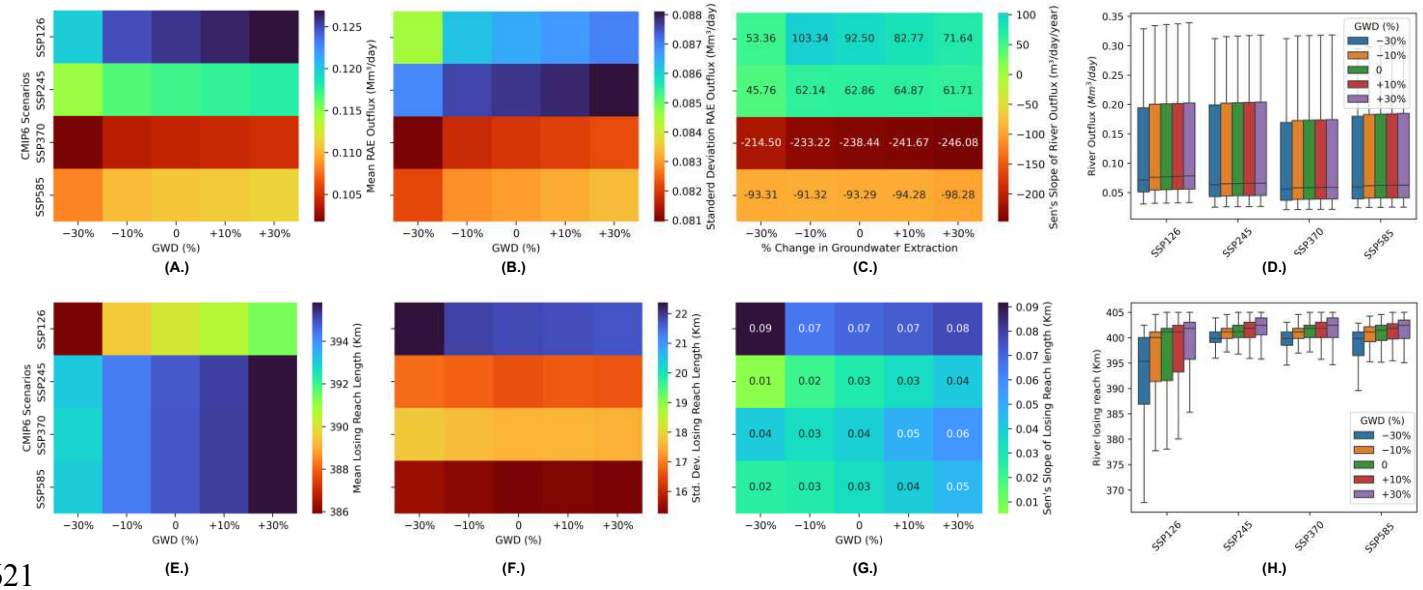


Figure 13. Scenario plots based on the Figure 2; Top row represents the statistics (A. Mean, B. Standard deviation, C. Sen's Slope/trend, and D. Summary box plots) for RAE outflux; The bottom row represents the statistics (E. Mean, F. Standard deviation, G. Sen's Slope and D. Summary box plot) for total loosing reach length of Varuna River.

I. **Green Growth Overreach**:

This quadrant, characterized by low climate pressure (SSP126/SSP245) but high development ambition and unsustainable groundwater use (+10% or +30% GWD), reveals a significant exacerbation of the Varuna River's losing stream characteristics. Despite favorable climatic conditions for recharge and river flow, the increased groundwater extraction drives a stronger hydraulic gradient from the river to the aquifer. Consequently, **Figure 13** shows an increased mean RAE outflux (e.g., up to 0.125 Mm³/day under SSP126/+30% GWD in **Figure 13**.A) and an expanded mean losing reach length (e.g., reaching 405 km under SSP126/+30% GWD in **Figure 13**.E). The Sen's Slope analysis reveals accelerating positive trends for both RAE outflux (e.g., 82.77 Mm³/day/year under SSP126/+30% GWD in **Figure 13**.C) and losing reach length (e.g., 0.08 km/year under

SSP126/+30% GWD in **Figure 13**.G). Furthermore, in **Figure 14**, +10% GWD and +30% GWD lines, representing increased abstraction, show slightly positive or near-zero deviations from the BAU baseline. This indicates the complete disconnection of river from the aquifer leading a constant seepage from the river bottom with no trends corresponding to increasing demand.

II. Hydro-Stress Collapse:

This quadrant, depicting high climate pressure (SSP370/SSP585) combined with increased groundwater exploitation (+10% or +30% GWD), represents the most extreme and detrimental impacts on the Varuna River's losing stream dynamics. The combined effects of reduced natural recharge (due to high climate pressure) and amplified hydraulic gradients from increased pumping led to the most severe river water loss. **Figure 13** shows the highest mean RAE outflux values (e.g., exceeding 0.125 Mm^3/day under SSP585/+30% GWD in **Figure 13**.A) and the longest mean losing reach lengths (e.g., surpassing 405 km under SSP585/+30% GWD in **Figure 13**.E). The long-term trends are overwhelmingly positive and reach their most alarming rates. For instance, the Sen's Slope for RAE outflux (**Figure 13**.C) shows rapidly increasing outflux (e.g., -98.28 Mm^3/day/year under SSP585/+30% GWD), and the trend for losing reach length (**Figure 13**.G) indicates significant expansion. In **Figure 14**, the green and purple lines for SSP370/SSP585 again show positive or near-zero deviations in total river outflow. This suggests that under severe climate stress and higher abstraction, the river losses its connection to the aquifer, leading to steady seepage to the aquifer.

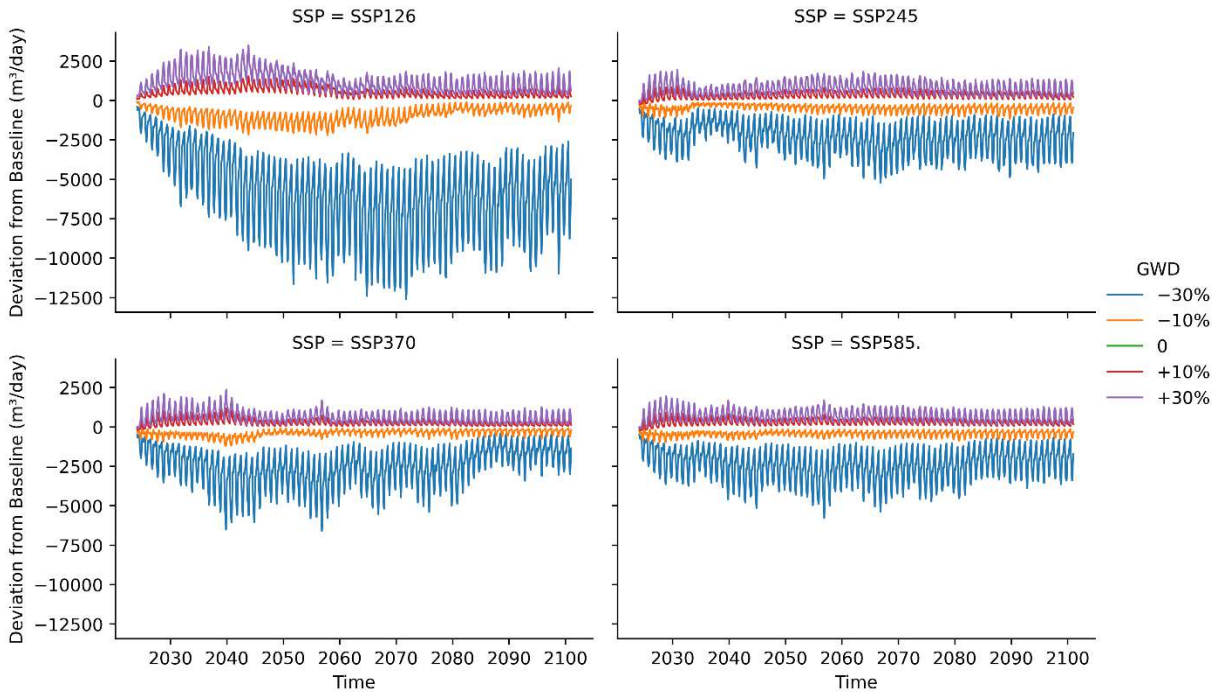
III. Sustainable Resilience:

This quadrant, representing low climate pressure (SSP126/SSP245) and proactive groundwater management (-10% or -30% GWD), yields the most beneficial outcomes for mitigating the Varuna River's losing stream characteristics. By reducing groundwater abstraction, the hydraulic gradient from the river to the aquifer is weakened, allowing more water to remain in the river. **Figure 13** shows the lowest mean RAE outflux values (e.g., 0.105 Mm^3/day under SSP126/-30% GWD in **Figure 13**.A) and the shortest mean losing reach lengths (e.g., 386 km under SSP126/-30% GWD in **Figure 13**.E). Critically, this quadrant uniquely exhibits negative long-term trends for both RAE outflux (e.g., -53.36 Mm^3/day/year under SSP126/-30% GWD in **Figure 13**.C) and losing reach length (e.g., -0.09 km/year under SSP126/-30% GWD in **Figure 13**.G). This demonstrates that strategically reducing groundwater abstraction (as per logistic growth of demand) under milder climate change actively reduces the rate of river water loss and effectively shortens the extent of losing reaches. Confirming this, **Figure 14** show significant negative deviations from the BAU baseline. This indicates a substantial reduction in total river outflow compared to BAU. This is consistent: by reducing pumping, less water is drawn from the aquifer, which means the river's ability to discharge (outflow) is reduced because there is less overall water in the system, or a shift towards more gaining reaches (reducing net loss to aquifer) means less water is 'leaving' the river system via aquifer loss. This implies a healthier and more naturally flowing river.

IV. Fragile Adaptation:

This quadrant portrays a future with high climate pressure (SSP370/SSP585) where groundwater reduction occurs, but its benefits are tempered by the challenging climate context. Despite reduced abstraction, the high climate pressure still promotes conditions

conducive to river water loss. Mean RAE outflux (**Figure 13**.A) and mean losing reach length (**Figure 13**.E) are notably higher than in the "Sustainable Resilience" quadrant but lower than in the high abstraction scenarios. For example, under SSP585/-30% GWD, mean RAE outflux is around 0.115 Mm^3/day and mean losing reach length is around 398 km. While the long-term trends (**Figure 13**.C, G) for reducing river loss are more favorable than with increased pumping, they are less pronounced or even become positive compared to the "Sustainable Resilience" quadrant. **Figure 14** show substantial negative deviations in total river outflow from BAU, consistent with reduced abstraction leading to less river loss to the aquifer. This signifies that while reducing abstraction helps mitigate the severe impacts of high climate pressure on losing stream dynamics, the overall effectiveness in reversing river water loss trends is diminished, resulting in only modest improvements in reducing river water loss compared to optimal conditions. Adaptation in this scenario is fragile, as the system struggles against inherent climatic stressors.



699

700 **Figure 14**. The increase/decrease in the net outflux from the Varuna River with respect to BAU for all SSPs

701

702 Collectively, this analysis establishes groundwater extraction as the most sensitive parameter
703 influencing both gaining and losing stream dynamics in the Varuna River basin, higher than the
704 direct effects of varying climate change pathways. As demonstrated across all raster plots (**Figure**
705 **9**.A-G and **Figure 11**.A-G), changes in GWD (from -30% to +30%) consistently drive profound
706 and predictable shifts in RAE influx/outflux and gaining/losing reach lengths, with corresponding
707 effects on net river outflow (**Figure 12**). Increases in extraction consistently enhance stream
708 outflux and expand losing reaches (Hydro-Stress Collapse, Green Growth Overreach), driving the
709 river towards greater hydrological disconnection and water loss. Conversely, reductions in
710 extraction dramatically reverse these trends, decreasing RAE outflux and contracting losing
711 reaches while simultaneously boosting RAE influx and expanding gaining reaches (Sustainable

712 Resilience, Fragile Adaptation). These clear responses to GWD adjustments highlight that direct
713 human intervention via pumping management offers the most immediate and effective lever for
714 mitigating hydrological degradation in the Varuna River.

715 Beyond groundwater extraction's primary influence, the river-aquifer system's response to climate
716 change has shown complexity. While high-emission futures (SSP370/SSP585) generally create
717 tougher conditions (less groundwater flowing into the river, more flowing out), the exact impact
718 varies. For example, even under high climate stress, reducing groundwater pumping still helps
719 lessen river water loss, though not as much as under milder climate. This non-uniform response
720 highlights the intricate balance of changing precipitation, evapotranspiration, and river-aquifer
721 interaction. Such complexity underscores why detailed GCM-integrated models, like integrated
722 SWAT-MODFLOW setup, are essential. Simply assuming rising temperatures mean universally
723 "bad" outcomes for groundwater risks missing how the system actually behaves, including any
724 balancing effects or unique regional factors. Robust modeling, therefore, is crucial for
725 understanding these varied responses and developing effective, targeted adaptation plans.

726 **4.5 Limitation and future work**

727 The presented methodological framework has it caveats, arising due to the model limitations and
728 data scarcity. Due to absence of extensive historical dataset in the area, the numerical model runs
729 only for two year only (2022-2023) with warmup of five months in year 2021, and used for
730 forecasting up to 2100 with climate data. Although we have extensively applied a multistage
731 calibration and uncertainty analysis, the lack of data still introduces unknown uncertainty,
732 especially for long-term variability. Secondly, the ensemble has been used to represent the model
733 uncertainty only and has not been used for climate change forecasting due to computational

limitations. In the future, the model will be revised upon collecting extensive data in Varuna River basin for effective decision making.

5 CONCLUSION

The study establishes the benefit of using groundwater model to determine baseflow compared to the widely used baseflow separation methodologies. Further, an integrated modeling framework has been formulated to assess the combined impacts of climate change and groundwater extraction on the Varuna River's river-aquifer exchanges (RAE). Future climate projections from CMIP6 Global Climate Models, delineated into low (SSP126/245) and high (SSP370/585) climate pressure scenarios, served as inputs to a coupled SWAT-MODFLOW hydrological model. Four groundwater abstraction scenarios, representing ±10% and ±30% changes from a Business As Usual baseline (constant extraction rate as per historical demand), were then simulated. Key hydrological indicators, including river-aquifer exchange influx/outflux, and the length of gaining/losing stream reaches, were statistically analyzed to quantify mean changes, variability, and long-term trends across these combined future scenarios. The major conclusions drawn are as follows:

- **Small gaining reaches in Varuna River**: The river shows a dynamic interaction with the groundwater system and has been found in majorly losing state in the monsoon season and gaining in dry periods (pre-monsoon). The net contribution of RAE to the stream flow varies from ~2% to ~12%, depending upon wet and dry seasons, respectively and the length if gaining reaches comprise of less than 5% of total river length.

- **Groundwater Extraction Dominance**: Groundwater abstraction proved to be the most critical anthropogenic parameter, exerting a more significant and predictable influence on both gaining and losing river reaches and overall river-aquifer exchange than the specific climate change pathways.
- **Mitigation through Reduced Pumping**: Reducing groundwater abstraction consistently enhanced RAE influx, expanded gaining reaches, and decreased RAE outflux and losing reach lengths, offering a robust strategy for improving river hydrological health.
- **Exacerbation by Increased Pumping**: Conversely, increased groundwater abstraction consistently led to severe degradation, characterized by reduced RAE influx, expanded losing reaches, and an accelerating loss of river water to the aquifer.
- **Complex Climate Response**: The river-aquifer system's response to climate change is complex and heterogeneous. Detailed modeling is crucial for understanding these nuanced interactions and avoiding oversimplified assumptions.
- **Scenario-Specific Outcomes**: The Sustainable Resilience quadrant (low climate pressure, reduced abstraction) showed optimal outcomes, while Hydro-Stress Collapse (high climate pressure, increased abstraction) consistently represented the worst-case scenario for river health and connectivity.

It can be safely concluded that the Varuna River is on the verge of losing its dry flow due to climate change and increasing groundwater demand. Given that this study quantitatively demonstrates that reduced groundwater abstraction is the most effective strategy for enhancing baseflow and river connectivity, the implementation of Managed Aquifer Recharge (MAR) structures is strongly recommended as a primary mechanism to achieve these reductions and ensure the long-term sustainability of the Varuna River. This requires decision-making

778 frameworks for the MAR in Gangetic alluvium (such as Varuna River basin), with the specific
779 focus on groundwater storage enhancement as well as stream health management.

780

781 ## 6 STATEMENTS AND DECLARATIONS

782 **Author Contributions**

783 All authors contributed to the study conception and design. Material preparation, data collection,
784 modelling and analysis were performed by R.K, S.G and A.O. The first draft of the manuscript
785 was written by R. K and all authors commented on previous versions of the manuscript. All authors
786 read and approved the final manuscript.

787 **Competing Interests**

788 The authors have no relevant financial or non-financial interests to disclose.

789 **Data Availability**

790 All the data and models are can be available on request.

791

792 ## 7 ACKNOWLEDGEMENT

793 The authors gratefully acknowledge the Prime Minister's Research Fellowship (PMRF) for
794 supporting the doctoral studies of R.K. We also extend our gratitude to the Smart Lab on Clean
795 Rivers (SLCR), India, for funding the data collection campaign and providing essential
796 computational facilities.

8 REFERENCES

Asoka, A., Wada, Y., Fishman, R., Mishra, V., 2018. Strong Linkage Between Precipitation Intensity and Monsoon Season Groundwater Recharge in India. Geophys. Res. Lett. 45, 5536–5544. https://doi.org/10.1029/2018GL078466

Bajpai, M., Gaur, S., Kumar, R., Ohri, A., Piégay, H., 2023. Suitable sites for groundwater development: a capture map-based approach integrated with weighted overlay analysis. AQUA — Water Infrastructure, Ecosystems and Society 72, 1184–1197. https://doi.org/10.2166/aqua.2023.011

Baratelli, F., Flipo, N., Moatar, F., 2016. Estimation of stream-aquifer exchanges at regional scale using a distributed model: Sensitivity to in-stream water level fluctuations, riverbed elevation and roughness. J. Hydrol. (Amst). 542, 686–703. https://doi.org/10.1016/J.JHYDROL.2016.09.041

Bartsch, S., Frei, S., Ruidisch, M., Shope, C., Peiffer, S., Kim, B., Fleckenstein, J., 2014. River-aquifer exchange fluxes under monsoonal climate conditions. J. Hydrol. (Amst). 509, 601–614. https://doi.org/10.1016/J.JHYDROL.2013.12.005

Brunke, M., Gonser, T., 1997. The ecological significance of exchange processes between rivers and groundwater. Freshw. Biol. 37, 1–33. https://doi.org/10.1046/J.1365-2427.1997.00143.X

Carolli, M., Geneletti, D., Zolezzi, G., 2017. Assessing the impacts of water abstractions on river ecosystem services: an eco-hydraulic modelling approach. Environ. Impact Assess. Rev. 63, 136–146. https://doi.org/10.1016/j.eiar.2016.12.005

Chunn, D., Faramarzi, M., Smerdon, B., Alessi, D., 2019. Application of an Integrated SWAT–MODFLOW Model to Evaluate Potential Impacts of Climate Change and Water Withdrawals

on Groundwater–Surface Water Interactions in West-Central Alberta. Water (Basel). https://doi.org/10.3390/W11010110

Cooper, D.M., Wilkinson, W.B., Arnell, N.W., 1995. The effects of climate changes on aquifer storage and river baseflow. Hydrological Sciences Journal 40, 615–631. https://doi.org/10.1080/02626669509491448

Cui, T., Sreekanth, J., Pickett, T., Rassam, D., Gilfedder, M., Barrett, D., 2021. Impact of model parameterization on predictive uncertainty of regional groundwater models in the context of environmental impact assessment. Environ. Impact Assess. Rev. 90. https://doi.org/10.1016/j.eiar.2021.106620

Daily, G.C., Ehrlich, P.R., 2016. Socioeconomic Equity , Sustainability , and Earth ' s Carrying Capacity Author (s): Gretchen C . Daily and Paul R . Ehrlich Published by : Wiley Stable URL : http://www.jstor.org/stable/2269582 Accessed : 02-05-2016 21 : 48 UTC Your use of the JSTOR arc 6, 991–1001.

Dey, S., Raju, N.J., Gossel, W., Mall, R.K., 2023. Hydrogeochemical characterization and geochemical modeling for the evaluation of groundwater quality and health risk assessment in the Varuna River basin, India. Environ. Geochem. Health 45, 4679–4702. https://doi.org/10.1007/s10653-023-01521-y

Doherty, J., 2015. Calibration and Uncertainty Analysis for Complex Environmental Models. Watermark Numerical Computing, Brisbane, Australia.

Ellis, P.A., Mackay, R., Rivett, M., 2007. Quantifying urban river-aquifer fluid exchange processes: a multi-scale problem. J. Contam. Hydrol. 91 1–2, 58–80. https://doi.org/10.1016/J.JCONHYD.2006.08.014

Gaur, S., Kumar, R., Ohri, A., Mishra, S., Gond, A.K., Dwivedi, S.B., Jha, M., Chaturvedi, A., Singh, B.N., 2023. Study of hydrologically critical subbasins under climate change. Journal of Water and Climate Change 14, 1723–1740. https://doi.org/10.2166/wcc.2023.038

Hu, K., Ailihazi, W., Danierhan, S., 2023a. Ecological Base Flow Characteristics of Typical Rivers on the North Slope of Kunlun Mountains under Climate Change. Atmosphere (Basel). https://doi.org/10.3390/atmos14050842

Hu, K., He, J., Danierhan, S., Tuerxun, Y., 2023b. Sensitivity of river ecological baseflow to climate change in arid areas 10. https://doi.org/10.3389/fenvs.2022.1080810

Jan, C.D., Chen, T.H., Lo, W.C., 2007. Effect of rainfall intensity and distribution on groundwater level fluctuations. J. Hydrol. (Amst). 332, 348–360. https://doi.org/10.1016/j.jhydrol.2006.07.010

Janardhana Raju, N., Ram, P., Dey, S., 2009. Groundwater quality in the lower Varuna River basin, Varanasi district, Uttar Pradesh. Journal of the Geological Society of India 73, 178–192. https://doi.org/10.1007/s12594-009-0074-0

Jasechko, S., Seybold, H., Perrone, D., Fan, Y., Kirchner, J., 2021. Widespread potential loss of streamflow into underlying aquifers across the USA. Nature 591, 391–395. https://doi.org/10.1038/s41586-021-03311-x

Konrad, C., 2006. Location and timing of river-aquifer exchanges in six tributaries to the Columbia River in the Pacific Northwest of the United States. J. Hydrol. (Amst). 329, 444–470. https://doi.org/10.1016/J.JHYDROL.2006.02.028

Krause, S., Blume, T., Cassidy, N., 2012. Investigating patterns and controls of groundwater up-welling in a lowland river by combining Fibre-optic Distributed Temperature Sensing with observations of vertical hydraulic gradients. Hydrol. Earth Syst. Sci. 16, 1775–1792. https://doi.org/10.5194/HESS-16-1775-2012

Kumar, A., Agrawal, S., 2025. Assessment of Water Quality in the Varuna River, Varanasi: A Comprehensive Study. Journal for Research in Applied Sciences and Biotechnology 4, 118–123. https://doi.org/10.55544/jrasb.4.1.14

Kumar, R., Bhattacharjee, R., Gaur, S., Ohri, A., 2025. Groundwater sustainability in the Varuna river basin: impacts of climate change and population growth. Environ. Earth Sci. 84, 295. https://doi.org/10.1007/s12665-025-12213-4

Li, H., Wang, W., Fu, J., Chen, Z., Ning, Z., Liu, Y., 2021. Quantifying the relative contribution of climate variability and human activities impacts on baseflow dynamics in the Tarim River Basin, Northwest China. J. Hydrol. Reg. Stud. https://doi.org/10.1016/j.ejrh.2021.100853

Lu, M., Rogiers, B., Beerten, K., Gedeon, M., Huysmans, M., 2021. Exploring river–aquifer interactions and hydrological system response using baseflow separation, impulse response modelling and time series analysis in three temperate lowland catchments. Hydrol. Earth Syst. Sci. https://doi.org/10.5194/hess-2021-422

Macdonald, D., Dixon, A., Gooddy, D., 2018. Water and nitrate exchange between a managed river and peri-urban floodplain aquifer: Quantification and management implications. Ecol. Eng. https://doi.org/10.1016/J.ECOLENG.2018.09.005

McCallum, A.M., Andersen, M.S., Rau, G.C., Larsen, J.R., Acworth, R.I., 2014. River-aquifer interactions in a semiarid environment investigated using point and reach measurements. Water Resour. Res. 50, 2815–2829. https://doi.org/10.1002/2012WR012922

Mccallum, J.L., Cook, P.G., Berhane, D., Rumpf, C., Mcmahon, G.A., 2012. Quantifying groundwater flows to streams using differential flow gaugings and water chemistry. J. Hydrol. (Amst). 416–417, 118–132. https://doi.org/10.1016/j.jhydrol.2011.11.040

Miller, O., Miller, M.P., Longley, P., Alder, J., Bearup, L., Pruitt, T., Jones, D.K., Putman, A., Rumsey, C., McKinney, T., 2021. How Will Baseflow Respond to Climate Change in the Upper Colorado River Basin? Geophys. Res. Lett. 48. https://doi.org/10.1029/2021GL095085

Mishra, M., Raman, V.A.V., Prudhvi Raju, K.N., 2024. Flood Reduction and Prevention Possibilities in the Flood Plains: A Study of the Varuna River Basin in the Flood Plain of the Ganga River, Uttar Pradesh, India. Journal Of The Geological Society Of India 100, 1713–1720. https://doi.org/10.17491/jgsi/2024/174043

Mukherjee, A., Bhanja, S.N., Wada, Y., 2018. Groundwater depletion causing reduction of baseflow triggering Ganges river summer drying. Sci. Rep. 8, 12049. https://doi.org/10.1038/s41598-018-30246-7

Partington, D., Brunner, P., Simmons, C., Werner, A., Therrien, R., Maier, H., Dandy, G., 2012. Evaluation of outputs from automated baseflow separation methods against simulated baseflow from a physically based, surface water-groundwater flow model. J. Hydrol. (Amst). 458, 28–39. https://doi.org/10.1016/J.JHYDROL.2012.06.029

Ren, Y., Mishra, S., Lian, Y., Zhang, J., Jin, J., Zhang, K., Wang, W., Gao, Y., Guan, Y., Ling, M., Sun, X., 2025. Water stress exacerbated by altered flow pathways in the Tibetan plateau: A critical analysis. Environ. Impact Assess. Rev. 114. https://doi.org/10.1016/j.eiar.2025.107888

Ronayne, M., Roudebush, J.A., Stednick, J., 2017. Analysis of managed aquifer recharge for retiming streamflow in an alluvial river. J. Hydrol. (Amst). 544, 373–382. https://doi.org/10.1016/J.JHYDROL.2016.11.054

Schilling, O.S., Cook, P.G., Brunner, P., 2019. Beyond Classical Observations in Hydrogeology: The Advantages of Including Exchange Flux, Temperature, Tracer Concentration, Residence Time, and Soil Moisture Observations in Groundwater Model Calibration. Reviews of Geophysics 57, 146–182. https://doi.org/10.1029/2018RG000619

Singh, S., Singh, K.N., 2010. Physico-chemical analysis of sewage discharged into Varuna river at Varanasi. Current World Environment 5, 201–203. https://doi.org/10.12944/CWE.5.1.35

Tang, Q., Kurtz, W., Brunner, P., Vereecken, H., Hendricks Franssen, H.J., 2015. Characterisation of river-aquifer exchange fluxes: The role of spatial patterns of riverbed hydraulic conductivities. J. Hydrol. (Amst). 531, 111–123. https://doi.org/10.1016/j.jhydrol.2015.08.019

Tang, Q., Kurtz, W., Schilling, O.S., Brunner, P., Vereecken, H., Hendricks Franssen, H.J., 2017. The influence of riverbed heterogeneity patterns on river-aquifer exchange fluxes under different connection regimes. J. Hydrol. (Amst). 554, 383–396. https://doi.org/10.1016/j.jhydrol.2017.09.031

Taylor, R.G., Scanlon, B., Döll, P., Rodell, M., van Beek, R., Wada, Y., Longuevergne, L., Leblanc, M., Famiglietti, J.S., Edmunds, M., Konikow, L., Green, T.R., Chen, J., Taniguchi, M., Bierkens, M.F.P., MacDonald, A., Fan, Y., Maxwell, R.M., Yechieli, Y., Gurdak, J.J., Allen, D.M., Shamsudduha, M., Hiscock, K., Yeh, P.J.-F., Holman, I., Treidel, H., 2013. Ground water and climate change. Nat. Clim. Chang. 3, 322–329. https://doi.org/10.1038/nclimate1744

Unland, N.P., Cartwright, I., Daly, E., Gilfedder, B., Atkinson, A., 2015. Dynamic river–groundwater exchange in the presence of a saline, semi-confined aquifer. Hydrol. Process. 29, 4817–4829. https://doi.org/10.1002/hyp.10525

Vasilevskiy, P., Wang, P., Pozdniakov, S., Wang, T., Zhang, Y., Zhang, X., Yu, J., 2022. Simulating River/Lake–Groundwater Exchanges in Arid River Basins: An Improvement Constrained by Lake Surface Area Dynamics and Evapotranspiration. Remote Sens. (Basel). 14. https://doi.org/10.3390/rs14071657

Vergnes, J.P., Habets, F., 2018. Impact of river water levels on the simulation of stream–aquifer exchanges over the Upper Rhine alluvial aquifer (France/Germany). Hydrogeol. J. 26, 2443–2457. https://doi.org/10.1007/s10040-018-1788-0

White, J.T., Hunt, R.J., Fienen, M.N., Doherty, J.E., 2020. Approaches to highly parameterized inversion: PEST++ Version 5, a software suite for parameter estimation, uncertainty analysis, management optimization and sensitivity analysis, Techniques and Methods. Reston, VA. https://doi.org/10.3133/tm7C26

Wöhling, T., Gosses, M., Wilson, S., Davidson, P., 2018. Quantifying River-Groundwater Interactions of New Zealand's Gravel-Bed Rivers: The Wairau Plain. Groundwater 56. https://doi.org/10.1111/gwat.12625

Xiang, Y., Wang, Y., Chen, Y., Zhang, Q., 2021. Impact of Climate Change on the Hydrological Regime of the Yarkant River Basin, China: An Assessment Using Three SSP Scenarios of CMIP6 GCMs. Remote. Sens. 14, 115. https://doi.org/10.3390/rs14010115

Zhang, R., Li, Q., Chow, T.L., Li, S., Danielescu, S., 2013. Baseflow separation in a small watershed in New Brunswick, Canada, using a recursive digital filter calibrated with the conductivity mass balance method. Hydrol. Process. 27. https://doi.org/10.1002/hyp.9417

Supplementary Files

This is a list of supplementary files associated with this preprint. Click to download.

- supplimentarydata.docx